1951

Investigation and calibration of a direct reading fluid flowmeter

Cummings, Handford Lindsley; Mallick, Edgar Eugene

Massachusetts Institute of Technology

INVESTIGATION AND CALIBRATION OF A DIRECT READING FLUID FLOWMETER

HANDFORD LINDSLEY CUMMINGS
EDGAR EUGENE MALLICK

INVESTIGATION AND CALIBRATION OF A DIRECT READING FLUID FLOWMETER

by

HANDFORD LINDSLEY CUMMINGS

B.S., United States Military Academy
(1945)

and

EDGAR EUGENE MALLICK

B.S., United States Naval Academy
(1943)

B.S.A.E., United States Naval Postgraduate School
(1950)

SUBMITTED IN PARTIAL FULFILLMENT OF THE
REQUIREMENTS FOR THE DEGREE OF
MASTER OF SCIENCE

at the

MASSACHUSETTS INSTITUTE OF TECHNOLOGY
(1951)

INVESTIGATION AND CALIBRATION OF A DIRECT READING FLUID FLOWMETER

by

H.L. Cummings and E.E. Mallick

Submitted for the degree of Master of Science in the Department of Aeronautical Engineering on May 18, 1951.

Summary

A flowmeter designed to directly measure mass flow as a function of the pressure difference across a rotating cylinder in a fluid stream was investigated. Calibration curves for the meter indicate an accuracy of measurement of two per cent. The useful range of the meter was found to be limited by the ratio of the cylinder tangential speed to the free stream velocity.

Cambridge, Massachusetts
May 18, 1951

Professor Joseph S. Newell
Secretary of the Faculty
Massachusetts Institute of Technology
Cambridge, Massachusetts

Dear Professor Newell:

We submit herewith our thesis entitled "Investigation and Calibration of a Direct Reading Fluid Flowmeter", in partial fulfillment of the requirements for the degree of Master of Science in Aeronautical Engineering.

ACKNOWLEDGEMENT

The authors wish to express their gratitude to Professor E.S. Taylor for his help and suggestions in the development of this investigation, and to the staff of the Gas Turbine Laboratory for their generous cooperation and assistance.

TABLE OF CONTENTS

INVESTIGATION AND CALIBRATION OF A DIRECT READING FLUID FLOWMETER

I. INTRODUCTION

A meter which would directly indicate the mass rate of fluid flow in a duct would have many engineering applications. The present standard flowmetering devices (the venturi meter, nozzle, and orifice) require the measurement of three stream properties and the computation of the mass rate of flow by use of an equation and various calibration coefficients. The problem of the metering of a fluid would, therefore, be greatly simplified if an indication of mass rate of fluid flow could be obtained from a direct reading instrument. Such a device would be of use in the control of fuel-air ratios under conditions of varying density as experienced in altitude operations of aircraft and missiles. In measuring the mass flow rate of gases of varying density or of unknown composition such a meter might be employed.

The purpose of this thesis is, then, the investigation, calibration, and analysis of such a direct read-

ing flowmeter.

The flowmeter upon which this report is based was designed and constructed by Tennant and Turner and reported upon in their thesis [1] * at the Massachusetts Institute of Technology in 1950. The original equipment has been modified by the present authors and this report includes results obtained from the operation of the modified apparatus and analysis of these results.

The flowmeter discussed in this report consists essentially of a square duct within which a cylinder rotates in a counter-clockwise direction about an axis perpendicular to the direction of flow as shown in Fig. 1. There is, consequently, a speeding up of the flow in the duct below the cylinder and a retardation of velocity above the cylinder. This difference in velocity results in a difference in static pressure at the walls of the duct directly above and below the rotating cylinder. The magnitude of this pressure difference is directly related to the mass flow in the duct as will be further discussed in Chapter II.

The principle upon which this device is based, that of a rotating object in a fluid stream, was originally

---

* Numbered superscripts refer to the Bibliography, p. 40 and 41.

discussed by Magnus [2] in 1851 in connection with the flight of projectiles and for this reason is generally known as the "Magnus Effect". The problem was also further discussed by Lord Rayleigh [3] in 1877 and by Lafay [5] in Paris in 1912. In the early 1920's the rotating cylinder was considered by many aerodynamicists as a more promising lifting device than the presently accepted and proven Joukowski airfoil. This outlook was based primarily on the potential flow analysis of the problem which theoretically predicts a lift coefficient for a rotating cylinder of 4π which is considerably higher than that obtained from airfoils of the Joukowski type. An explanation of this analysis is given by Goldstein [4].

Extensive experimentation was carried out at the German laboratories at Gottingen under the direction of Prandtl [19, 24]. Flow pictures obtained by Prandtl are shown in Fig. 17 and are discussed in detail in later pages of this report.

The promising results obtained at Gottingen led Flettner to apply the principle of the "Magnus Effect" to ship propulsion; replacing the sails with two 45 ft. high, 9 ft. in diameter, rotating cylinders. The Flettner rotor ship made several semi-successful runs;

however, the question of the practicability of such a mode of propulsion was a source of much controversy. Two papers by Betz [11] and Ahlborn [12] discuss the pros and cons of the Flettner rotor ship.

Concurrent with the Gottingen experimentation, considerable research concerning the rotating cylinder in a real fluid was carried out by Thom [6,7,8] in England.

With the failure of the Flettner rotor ship to fulfill the expectations of its designers, a consequent lack of interest in the rotating cylinder as a lifting device resulted. In 1925 Reid [9] of the NACA described experiments with a rotating cylinder in an airstream which confirmed much of the data obtained by other investigators.

To date the practical applications of the lifting force obtained from the "Magnus Effect" have been largely unsuccessful. Perhaps the information presented in this report will result in a practical employment of this long known and much studied phenomenon.

II. THEORETICAL ANALYSIS

2.1 Introduction. The development of the theoretical flowmeter equation contained in this chapter follows substantially the original derivation as set forth by Tennant and Turner [1]. This treatment is included in this report, however, both for completeness and for correction of a few minor errors, notably an error in the calculation of the numerical constant in the theoretical flowmeter equation of the original thesis. The method followed in the derivation is essentially an extension and combination of two analyses as reported by Durand [10].

The meter is basically as shown in Fig. 1. By measuring the pressure difference ΔP between points A and B when the cylinder is rotating at a known constant speed it is proposed to measure the mass rate of flow through the apparatus. For realization of such a meter there must exist a relation of the form

$$M_a = \text{const.} \times \Delta P \qquad (1)$$

where M_a denotes the mass rate of flow. Expressing M_a as the product of ρ, density; A, area; and V, velocity we obtain $\rho AV = \text{const.} \times \Delta P$

which, with a known constant meter geometry, may be expressed as

$$\Delta P = const \times \rho V \qquad (2)$$

Thus it remains to demonstrate the existence of relation (2) and to obtain a numerical value for the constant of relation (1).

For the accomplishment of the above aims several simplifications of the actual flow are assumed:

a. The flow is two dimensional.

b. The flow is irrotational.

c. The fluid is a non-viscous, incompressible, ideal fluid.

d. The rotating cylinder imparts to the fluid a circulation Γ, equal to 2π times the product of the radius, R, of the cylinder, and the peripheral speed, U, of the cylinder.

The above assumptions, combined with the requirement that the flow be continuous, make possible the employment of the theory of potential flow for synthesis of the flow pattern within the meter. Having an expression which describes the flow in the meter, it is then possible to find the velocities at points A and B. With

these velocities known, the Bernoulli equation is applied between the two points resulting in an expression relating the difference in pressure between A and B to the stream velocity and density.

2.2 Method of Analysis. The potential flow pattern about a stationary cylinder in a fluid stream is produced by combination of a source-sink doublet and parallel flow (Fig. 2a). If a potential vortex, the core of which is the cylinder (Fig. 2b), is added to this picture, the flow pattern for a rotating cylinder in an unrestrained fluid stream is the result (Fig. 2c). In the actual meter the flow is restrained by the walls of the meter duct. The effect of the walls upon the flow pattern is simulated by the method of images originally devised by Glauert [26]. The wall correction is applied separately to the flow patterns of the stationary cylinder (Fig. 3a) and the potential vortex (Fig. 3b). The superposition of these two corrected patterns is then the true potential flow pattern for the meter.

2.3 The Stationary Cylinder and Its Images. Consider the complex z plane with x and iy axes as shown in Fig. 3a. The complex variable $z = x + iy$ describes any point in this plane. The stationary cylinder is located with

center at the origin. The effects of the duct walls on the flow are simulated by an infinite series of cylinder images extending in both positive and negative directions. Centers of the image cylinders are located on the iy axis at $iy = \pm ink$ where n is a positive integer and k is the duct height.

The potential function $F = \phi + i\psi$ completely describes any potential flow. ϕ, the velocity potential, ψ, the stream function, and F are functions of the complex variable z. The potential function for the flow about a stationary cylinder in a parallel stream of velocity V is *

$$F = Vz + \frac{C}{z} \qquad (3)$$

where C is a constant. This function describes the flow at any point z in the complex plane due to the obstructing cylinder at the origin. Similarly

$$F = Vz + \frac{C}{z - ink}$$

---

* Hildebrand, Ref. 13, p. 547, Eq. 174.

describes the flow at any point z due to a cylinder image at iy = + ink and

$$F = Vz + \frac{C}{z + ink}$$

describes the flow at z due to a cylinder image at iy = − ink. The potential function for the collectivity of images and real cylinder is then

$$F = Vz + C\left[\frac{1}{z} + \sum_{1}^{\infty}\left(\frac{1}{z - ink} + \frac{1}{z + ink}\right)\right] \quad (4)$$

Making the substitution $C = C_1 \frac{K}{\pi}$ and simplifying:

$$F = Vz + C_1\left\{\frac{1}{\left(\frac{\pi z}{K}\right)} + 2\left(\frac{\pi z}{K}\right)\sum_{1}^{\infty}\left[\frac{1}{\left(\frac{\pi z}{K}\right)^2 + n^2\pi^2}\right]\right\}$$

The sum of which, by Mittag-Leffler's theorem *, is

$$F = Vz + C_1 \coth\frac{\pi z}{K} \quad (5)$$

---

* Jeffreys and Jeffreys, Ref. 14, p. 357, Eq. 8.

The stream velocity w at z is given by the derivative $\frac{dF}{dz}$ at that point

$$w = \frac{dF}{dz} = V - \frac{C_1 \frac{\pi}{K}}{\sinh^2 \frac{\pi z}{K}} \tag{6}$$

To evaluate C_1, consider the physical condition that the velocity is zero at the points on the x axis where $z = \pm R$, R being the radius of the cylinder. Then

$$C_1 = \frac{KV}{\pi} \sinh^2 \frac{\pi R}{K}$$

The velocity at any point z is then

$$w = V\left(1 - \frac{\sinh^2 \frac{\pi R}{K}}{\sinh^2 \frac{\pi z}{K}}\right) \tag{7}$$

At the walls directly above and below the cylinder where $z = \pm i\frac{K}{2}$, the velocity is

$$w = V\left(1 - \frac{\sinh^2 \frac{\pi R}{K}}{\sinh^2 \pm i\frac{\pi}{2}}\right)$$

which reduces to

$$w = V\left(1 + \sinh^2 \frac{\pi R}{K}\right) \qquad (8)$$

which is the velocity at points A and B on the walls, directly above and below the cylinder, due to the obstruction to the flow by the cylinder. To this must be added the velocity due to the rotation of the cylinder.

2.4 The Vortex and Vortex Images. Again consider the complex plane as shown in Fig. 3b. The circulation supplied to the fluid by the rotation of the cylinder is represented by a potential vortex at the origin, the core of which is the cylinder. The effect of the duct walls is simulated by an infinite series of vortex images located on the iy axis with centers at iy = $\pm$ ink. To give the correct velocity distribution transverse to the flow direction, alternate vortices are given opposite

rotations; therefore, there is a distance 2k between vortices of the same circulation.

The potential function at any point z for a vortex located at the origin is *

$$F = \frac{-i\Gamma}{2\pi} \ln z = \frac{\Gamma}{2\pi i} \ln z \qquad (9)$$

where Γ, the circulation, is positive in the counter-clockwise direction.

It will be mathematically convenient if we sum velocity expressions, therefore, taking the derivative

$$W = \frac{dF}{dz} = \frac{\Gamma}{2\pi i} \frac{1}{z} \qquad (10)$$

which is the velocity at any point z due to a vortex of strength Γ located at the origin.

The velocity at any point z due to a vortex of same direction of rotation located at iy = + in2k is

$$W = \frac{\Gamma}{2\pi i} \frac{1}{z - i n 2K}$$

---

* Hildebrand, Ref. 13, p. 545, Eq. 172.

The velocity at any point z due to a vortex of same rotation at iy = -in2k is

$$W = \frac{\Gamma}{2\pi i} \quad \frac{1}{z + i n 2k}$$

The sum of the velocities at z due to the real vortex and a positive and negative infinite series of vortices of the same direction of rotation is

$$W = \frac{\Gamma}{2\pi i}\left\{\frac{1}{z} + \sum_{1}^{\infty}\left[\frac{1}{z - i n 2k} + \frac{1}{z + i n 2k}\right]\right\} \qquad (11)$$

Making the substitution $\Gamma = \Gamma_1 4K$, and simplifying:

$$W = \frac{\Gamma_1}{i}\left\{\frac{1}{\left(\frac{\pi z}{2K}\right)} + 2\left(\frac{\pi z}{2K}\right)\sum_{1}^{\infty}\left[\frac{1}{\left(\frac{\pi z}{2K}\right)^2 + n^2\pi^2}\right]\right\}$$

The sum of which by Mittag-Leffler's theorem * is

$$W = \frac{\Gamma_1}{i} \coth \frac{\pi z}{2K} \qquad (12)$$

---

* Jeffreys and Jeffreys, Ref. 14, p. 357, Eq. 8.

Rewriting in terms of Γ :

$$W = \frac{\Gamma}{4Ki} \coth \frac{\pi z}{2K} \qquad (13)$$

which is the velocity at any point z due to the real vortex and the infinite series of images of same direction of rotation.

To this must be added the velocity due to the images of opposite rotation.

The velocity at z due to a vortex of opposite rotation at $iy = +i(2n-1)K$ is

$$W = \frac{-\Gamma}{2\pi i} \quad \frac{1}{z - i(2n-1)K}$$

The velocity at z due to a vortex of opposite rotation at $iy = -i(2n-1)K$ is

$$W = \frac{-\Gamma}{2\pi i} \quad \frac{1}{z + i(2n-1)K}$$

The sum of the velocities at z due to the positive and negative infinite series of vortices of opposite rotation is

$$W = \frac{-\Gamma}{2\pi i} \sum_{1}^{\infty} \left[\frac{1}{z - i(2n-1)K} + \frac{1}{z + i(2n-1)K} \right] \qquad (14)$$

Making the substitution $\Gamma = \Gamma_1 4K$, and simplifying:

$$W = \frac{-\Gamma_1}{i} \delta\left(\frac{\pi z}{2K}\right) \sum_{1}^{\infty} \left[\frac{1}{4\left(\frac{\pi z}{2K}\right)^2 + (2n-1)^2 \pi^2} \right]$$

The sum of which, again by Mittag-Leffler's theorem *, is

$$W = \frac{-\Gamma_1}{i} \tanh \frac{\pi z}{2K} \qquad (15)$$

Rewriting in terms of Γ :

$$W = \frac{-\Gamma}{4Ki} \tanh \frac{\pi z}{2K} \qquad (16)$$

which is the velocity at z due to the infinite series of vortices of opposite rotation.

Combining equations (13) and (16) the total ve-

---

* Jeffreys and Jeffreys, Ref. 14, p. 357, Eq. 11.

locity at any point z due to the real vortex and all its images is

$$W=\frac{\Gamma}{4Ki}\left[\coth\frac{\pi z}{2K}-\tanh\frac{\pi z}{2K}\right] \qquad (17)$$

which can be simplified to

$$W=\frac{\Gamma}{2Ki}\left(\frac{1}{\sinh\frac{\pi z}{K}}\right) \qquad (18)$$

At point A on the wall directly above the cylinder $z = +i\frac{K}{2}$ and the velocity due to the vortex and wall effect upon the vortex is

$$W=-\frac{\Gamma}{2K} \qquad (19)$$

Similarly at point B the velocity is

$$W=+\frac{\Gamma}{2K} \qquad (20)$$

To these velocities must be added the velocity due to the stationary cylinder and its images. Combining equations (8) and (19) and replacing Γ by $2\pi RU$ we

obtain for the total velocity at A:

$$W_A = V\left(1+\sinh^2\frac{\pi R}{K}\right) - \frac{\pi R}{K}U \qquad (21)$$

Combining equations (8) and (20) and similarly replacing Γ we obtain for the total velocity at B:

$$W_B = V\left(1+\sinh^2\frac{\pi R}{K}\right) + \frac{\pi R}{K}U \qquad (22)$$

2.5 Theoretical Flowmeter Equation. With the velocities at points A and B known, we apply the Bernoulli equation between points A and B.

$$\Delta P = \frac{\rho}{2g}\left(W_B^2 - W_A^2\right) \qquad (23)$$

which results in

$$\Delta P = \frac{\rho}{2g}\,\frac{4\pi R}{K}\,UV\left(1+\sinh^2\frac{\pi R}{K}\right) \qquad (24)$$

Equation (24) with a constant speed of cylinder rotation is of the form

$$\Delta P = \text{const.} \times \rho V \qquad (2)$$

which establishes the theoretical basis for the flowmeter.

Combining equation (24) with the usual equation for mass flow and substituting the dimensions of the meter we arrive at the theoretical flowmeter equation

$$M_a = .155 \times 10^4 \frac{\Delta P}{N} \qquad (25)$$

in which M_a is in lbm/sec, ΔP is in inches of water, and N is the revolutions per minute of the cylinder.

III. EQUIPMENT AND PROCEDURE

The flowmeter investigated consisted of an aluminum cylinder four inches in diameter mounted in an eight inch square duct as shown schematically in Fig. 1. Annular aluminum end plates were inserted in the sides of the duct walls to house the ends of the cylinder. This arrangement of end plates was provided to eliminate the flow of air around the ends of the cylinder; thus simulating two dimensional flow. The shaft ends of the cylinder were fitted into New Departure, S.K.F. No. 2, self-aligning ball bearings. In order to assure accurate alignment of the cylinder within the duct walls, the races of the ball bearings were housed in four inch square, 1/4 inch thick, aluminum plates that were attached to the duct walls. The photograph in Fig. 4 shows the details of the cylinder mounting in a cut away view of the test section. Since sealed ball bearings were not used, some leakage of air was expected around the cylinder shaft. During the test runs, however, the pressure in the test section was held as closely as possible to atmospheric in order to minimize leakage.

The cylinder shaft was extended through the test section wall on the power input side, and coupled to the

power drive by means of a flexible coupling. The photograph in Fig. 5 shows the details of the power drive installation.

A standard Dumore No. 5, 1/2 h.p. grinding motor was used to rotate the cylinder. The quill of the grinding motor was coupled to the cylinder shaft as shown in Fig. 5. The Dumore No. 5 grinding motor was chosen to drive the cylinder because it afforded a suitable range of rotational speeds (up to 14,000 RPM for the equipment used) for testing purposes. Since accurate alignment of the driving motor quill with the cylinder shaft was necessary in order to eliminate vibration problems, the motor was mounted on a bracket that afforded easy adjustment for alignment purposes. The motor mounting bracket permitted adjustment in two directions at right angles to each other in the horizontal plane. A vertical adjustment on the driving motor permitted alignment in the vertical direction. Positive control of the RPM of the motor was obtained by controlling the voltage input to the motor with a Variac. The RPM of the cylinder was measured with a Strobotac.

Air for the flowmeter was supplied in a closed circuit system by the DeLaval Air Compressor of the M.I.T. Gas Turbine Laboratory. This compressor is normally

used for the Gas Turbine Laboratory variable density wind tunnel and is rated at 15,500 ft.^{3}/min.. Supply and return of air to the flowmeter was afforded by means of a ten and one-fourth inch spirally welded pipe. A plan view of the layout is shown in Fig. 6, and a photograph of the installation is shown in Fig. 7.

In conducting the tests it was found to be more practicable to run the cylinder at a constant RPM, and to vary the air flow. Seven different RPMs were selected for making the test runs: 3,300; 4,350; 6,400; 8,700; 10,000; 12,000; and 14,000. The selection of these RPMs was arbitrary; they were chosen to illustrate the effect of RPM on flow measurement for this type of flowmeter. The dependence of the flowmeter on the ratio of cylinder tangential speed to free stream velocity for accurate flow measurement is discussed in Chapter IV.

Calibration of the flowmeter was effected by use of a standard ASME square edged orifice which was placed in the flow circuit as shown in Fig. 6. The diameter ratio of this orifice was 0.6. Calibration curves for the orifice are shown in Appendix II. The pressure difference across the orifice was measured with a water manometer at low air flows with a means provided for switching to a mercury manometer at high air flows.

Screens and brass flow-straightening tubes of two inch outside diameter were placed in the flow circuit at two places (see Fig. 6) so that parallel flow conditions would be more closely approximated upstream of the flowmeter and the orifice.

The mass flow of air was varied from approximately 0.6 lb./sec. to 6 lb./sec. for each test run. For the equipment used, this mass flow of air corresponds to free stream velocities varying from approximately 20 ft./sec. to 190 ft./sec.. The highest free stream velocity corresponds to a Mach Number of approximately .17. It is assumed, therefore, that compressibility effects were negligible. The flow Reynolds Number (based on the diameter of the orifice) varied from $.14 \times 10^6$ to 1.2×10^6 for the range of free stream velocities used for these tests.

Two different locations of the static pressure taps for measuring the pressure difference across the rotating cylinder of the flowmeter were investigated. One location was in the duct walls directly above and below the center of the cylinder as shown schematically in Fig. 1 as points A and B. The authors were guided in their assumption that this was the optimum location * for

---

* Betz, Ref. 11, p. 18.

the taps since Prandtl reported in his experiments with rotating cylinders that theoretical potential flow conditions were more closely approximated in this region. The pressure taps located in this position are referred to in this report as the primary pressure taps. The second location investigated was at the end of the cylinder with the taps diametrically opposed at the surface of the cylinder. The pressure taps located in this position are referred to as the secondary pressure taps. The location of these taps is shown schematically in Fig. 1 at points C and D.

The pressure difference from the primary taps was read on an Ellison Inclined Vertical Draft Gauge which was calibrated to read pressure difference directly in inches of water. Since the range of this instrument extended only to 12 inches of water provisions were made for switching to a conventional water manometer when larger readings were necessary. A photograph of the manometer board used for taking readings is shown in Fig. 3.

Pressure difference from the secondary taps was read on a conventional water manometer.

In order to provide a means for evaluating static pressure loss across the flowmeter, static pressure taps

were installed 12 inches upstream and 12 inches downstream from the rotating cylinder as shown in Fig. 6 . The difference in pressure was measured on a conventional water manometer.

In the test procedure the cylinder was rotated at a selected RPM. This RPM was kept as constant as possible throughout the run by using a Variac to control as necessary the voltage input to the motor. The mass flow of air through the system was started at as low a value as could be obtained with the test equipment and increased in selected increments. Simultaneous readings of all manometers were taken during each increment of air flow with sufficient time being allowed between readings for steady flow conditions to be established. The mass flow for each flow increment was computed from the orifice data, and the reading of the flowmeter was calibrated with this mass flow. The data taken and sample calculations are shown in Appendix I.

IV. DISCUSSION OF RESULTS

4.1 Introduction. A graphical analysis of the results of the investigation and calibration of the flowmeter is given in Figs. 9 through 16. Figs. 9, 10, and 11 present curves relating actual mass fluid flow and meter readings. These curves indicate the true worth of the apparatus. Figs. 12, 13, and 14 present plots involving various parameters and non-dimensional quantities. These curves are offered in partial explanation of the results portrayed in the first group of plots. These curves also show the limitations of the meter and offer guidance in selecting the meter characteristics for an expected range of mass flow. Figs. 15 and 16 present other data obtained in the course of this investigation.

4.2 The Velocity Ratio U/V. The non-dimensional velocity ratio U/V is a quantity which figures extensively in correlation and explanation of meter data. In this ratio, U denotes the peripheral velocity of the rotating cylinder, while V denotes the free undisturbed stream velocity ahead of the meter. That the factor U/V exerts a great influence on the flow picture within the meter is demonstrated both from potential flow theory and from consideration of real fluid flow phenomena. The potential flow

pattern for a stationary cylinder in parallel flow as shown in Fig. 2a is, in effect, the flow pattern for a U/V of zero. The flow stagnation points are seen to exist exactly at the front and rear of the cylinder. If a circulation is added, U/V becomes a positive quantity and the stagnation points move along the surface of the cylinder closer to the region of decreased velocity as is pictured in Fig. 2c. Further increases in circulation, that is, further increases in U/V, result in junction of the two stagnation points on the underside of the cylinder and movement of the stagnation point into the fluid. The effect of the ratio U/V on the flow pattern of a real fluid can be clearly seen in Fig. 17 which is a series of flow pictures taken by Prandtl at Gottingen. For values of U/V at which the flow picture of the real viscous fluid resembles the potential flow pattern, correct indications by the flowmeter should be expected. When, however, the viscous effects are such as to cause complete disagreement between the actual pattern and the pattern of the potential flow, we should expect that our meter reading will not be an indication of the actual mass flow. Examination of Fig. 17 would lead us to expect no worthwhile meter indications below a U/V of about one.

This critical value of U/V cannot be applied di-

rectly to our flowmeter, however, due to the difference in measurement of the quantity V. The Prandtl pictures are of a cylinder rotating in an unrestrained fluid stream. The flowmeter stream is considerably restrained by the duct walls; consequently, the true V is greater than the free stream V used in computing the U/V of this report. Thom[6] gives a method for correction of U/V to include duct wall influence; however, the authors doubt the validity of the approximations made and have omitted any corrections to U/V in this paper. Thus, the actual values of U/V computed in this report may not be compared with values obtained by other investigators, but U/V still remains an important parameter for correlation of flowmeter data at various cylinder rotational speeds and mass flow rates.

That the ratio U/V is a determining factor in flowmeter performance may be deduced in another manner. In problems of flow similitude, the Reynolds Number, which is the ratio of inertia forces to viscous forces, has been theoretically and experimentally shown to be a controlling parameter. The flow in the meter may be considered as the superposition of two flows, the parallel flow in the duct and the circulatory flow. The Reynolds Number for the duct flow may be written as

$$R_e = \frac{\rho V c}{\mu}$$

where ρ is the fluid density, V is the stream velocity, μ is the fluid viscosity, and c is the hydraulic diameter of the duct. The Reynolds Number for the circulatory flow may be written as

$$R_e = \frac{\rho U d}{\mu}$$

where U is the peripheral velocity of the cylinder and d is the cylinder diameter. Thus, for the same fluid and fixed meter geometry, the factor U/V is seen to be a ratio of Reynolds Numbers and hence viscous effects should be expected to be a function of U/V.

4.3 Discussion of Figs. 9, 10, and 11. Figs. 9, 10, and 11 are plots of actual mass flow, M_a, versus $\frac{\Delta P}{N}$ which is the meter reading in inches of water divided by the cylinder RPM. The abscissa is actually $\frac{\Delta P}{N} \times 10^4$ to enable the use of whole number scale divisions in plotting. The theoretical flowmeter equation derived in Chapter II

$$M_a = .155 \times 10^4 \frac{\Delta P}{N} \qquad (25)$$

is plotted on all three graphs as a dashed straight line.

Fig. 9 shows the performance of the meter as compared with the theoretical prediction for 5 RPMs, the highest of which is 10,000 RPM. The useful range for any RPM is represented by the nearly straight line portion of the curve extending outward from the origin. It can be observed that, at low RPMs, this useful range is extremely narrow and widens with increasing RPM. The curve for 10,000 RPM shows a range of useful operation up to a mass flow of about 3.9 lbm/sec .

Fig. 10 is a similar plot which shows the useful range of operation for an RPM of 12,000. Three independent runs made on different days are plotted on this graph to demonstrate the reproducibility of data. The three runs may be represented by a mean line up to a mass flow of about 4.6. This mass flow corresponds to a U/V of about 1.6 which will be shown in the discussion of the next section to be the critical value of U/V below which the meter is not accurate. Therefore, divergence of the data at this point as occurs on this graph is to be expected. Examination of the data for the three runs, for mass flows above the critical value of U/V, shows a maximum deviation of 2% from the mean line.

In Fig. 11 three separate runs at 14,000 RPM are

plotted. A maximum deviation of about 2% from the mean line is also found at this RPM.

Both Figs. 10 and 11 show decided depressions in the curves between mass flows of 1 and 2 lbm/sec . These depressions occur at high values of U/V of the order of 6 to 9. It is suspected that in this region a component of the flow velocity is directed into one or both of the static pressure taps, thus causing a slight irregularity in the calibration curves.

Figs. 9, 10, and 11 are the calibration curves for the flowmeter which might be used in actual operation; however, it is necessary to examine other plotted relations for further insight into the meter flow process.

4.4 Discussion of Fig. 12. The velocity ratio U/V is plotted versus $\frac{\Delta P}{N} \times 10^4$ in Fig. 12 for the seven RPMs which have been studied. Also plotted is the theoretically predicted line for 4,350 RPM. The theoretical curves for the other six RPMs have been omitted since they would conflict with the curves plotted from the actual data. The theoretical curves are a family of hyperbolas all similar to the curve for 4,350 RPM. According to the theoretical relation derived in Chapter II, $\frac{\Delta P}{N}$ is directly proportional to M_a , the mass rate of flow. With

a constant fluid density and duct area the velocity V is also directly proportional to the mass flow. For a constant RPM, U, the peripheral velocity, is a constant and U/V is thus proportional to $\frac{1}{Ma}$. $\frac{\Delta P}{N}$ is proportional to Ma ; therefore, we are, in effect, plotting a relation of the type "x versus 1/x" which is, of course, a hyperbola.

The actual curves are displaced from the theoretical curves due to the many simplifications of the flow made in the theoretical calculation. The curves for 10,000, 12,000, and 14,000 RPM very closely conform to the hyperbolic shape which is again an indication of their useful range of operation. The significant feature of Fig. 12 is that the curves for all RPM below 12,000 show a break at a U/V of about 1.6. This confirms the suspicion that the flow process within the meter is primarily dependent upon the value of the velocity ratio. Above the critical value of U/V the speed of rotation of the cylinder is sufficient to prevent separation of the boundary layer fluid from the cylinder and consequent formation of vortices. Here, then, the flow pattern still resembles the potential flow pattern. At the critical value of U/V the rotation of the cylinder is no longer sufficient to prevent boundary layer separation in the rear of the cylinder and consequently the flow picture is no longer

similar to that predicted by potential flow. Probably in this region of operation the static pressure taps at "A" and "B" no longer measure only static pressure but now recover a component of the velocity directed toward them in the turbulent and presently unpredictable flow which results when separation from the cylinder occurs. The flow pattern at and below this critical point is probably much like the photographs for U/V 's of 1/2 or 1 of Fig. 17. Stagnation of a component of the velocity in the pressure taps below the critical value of U/V is probably also the cause of the change in sign of the measured pressure difference which occurs for 3,300 RPM and which is shown on both Figs. 9 and 12.

4.5 Discussion of Fig. 13. Fig. 13 is a plot of calibration coefficient, K, versus U/V and is included here for academic consideration rather than for actual use in connection with flowmeter operation. For actual flowmeter operation, use of a calibration curve such as Fig. 11 is recommended. The calibration coefficient is defined as the ratio of the actual mass flow to the theoretical mass flow for a given value of $\frac{\Delta P}{N}$. Thus, it is a ratio of the instantaneous slope of the actual curves of Figs. 9, 10, and 11 to the slope of the theo-

retical flowmeter equation.

Below a U/V of 1.6 the values of K are meaningless and in many cases off the scale of this graph due to the predominance of viscous effects which bring about flow separation as discussed in the previous section. Above a U/V of 1.6 the data for various RPMs can not be said to plot as a single line; however, the general shape of the curves for all the RPMs is similar. At high U/V 's there appears to be more correlation of the data for different values of RPM. Above the critical value of U/V the calibration coefficient is of the order of 4. This means that the pressure difference obtained for a given mass flow and RPM is only one fourth of the theoretically predicted pressure difference.

This result is in close agreement with data obtained by Thom [7] who measured the circulation produced by a rotating cylinder at a U/V of 2. The results of this experiment are shown in Fig. 18 in which circulation is plotted versus radial distance from the surface of the cylinder. Thom found that the actual circulation imparted to the fluid at a small distance from the cylinder is equal to about .24 of the theoretical value and remains constant at this value further from the cylinder. Since the circulation ($\Gamma = 2\pi RU$) appears as a factor in

the theoretical equation for ΔP (Eq. 24, Chap. II), this would mean an expected reduction in ΔP to about one fourth of the original theoretical value. A value of K of about four is then to be expected from consideration of Thom's results.

Examination of Fig. 13 shows an increasing value of K at the higher values of U/V. This indicates that the actual pressure difference measured by the meter is less than the predicted pressure difference by an even greater amount than the condition discussed in the preceding paragraph. This further lowering of ΔP could possibly be due to a tilting of the flow pattern in the direction of flow. When the flow pattern is tilted, the meter pressure taps no longer measure the maximum pressure difference and consequently a higher value of calibration coefficient will be required. Tilting of the flow pattern at high values of U/V might also result in a component of the velocity into the pressure taps as previously discussed.

4.6 Discussion of Fig. 14. The non-dimensional quantity $\frac{\Delta P}{q}$ is plotted versus U/V in Fig. 14. q is the free stream dynamic pressure ($\frac{1}{2} \rho V^2$). Below a U/V of 1.6 there is no correlation of data for various RPMs as

expected; however, above the critical U/V, all the data for various RPMs appears in general to conform to one line. The factor $\frac{\Delta P}{q}$ is similar to the lift coefficient used to describe airfoil characteristics. Thom [6] plots lift coefficient versus U/V for a rotating cylinder and obtains a curve very similar in shape to that of Fig. 14. Similar curves are also reported by Goldstein [4] from data of other investigators. The factor U/V is actually a ratio of Reynolds Numbers as previously discussed. This curve is then not constructed for any specific flow Reynolds Number but includes many varied values of this parameter. From this curve it may be concluded that flow in the meter is not a function of the flow Reynolds Number but is dependent only upon the value of the velocity ratio U/V.

4.7 Discussion of Fig. 15. To investigate the optimum location of the meter pressure taps, secondary taps were installed close to the surface of the cylinder at one end of the cylinder (points "C" and "D" of Fig. 1). Curves of Ma versus $\frac{\Delta P}{N}$ for these taps were meaningless and are not included in this report. Fig. 15 shows U/V versus $\frac{\Delta P}{N}$ for these secondary pressure taps. The shape of the curves for the various RPMs is seen to

vary with U/V as before. Breaks in the curves appear at constant values of U/V which is another indication of the dependence of the flow upon this parameter.

4.8 Discussion of Fig. 16. The difference in static pressure ahead of and behind the flowmeter (12 inches in each direction) is plotted versus mass rate of flow in Fig. 16 for an RPM of 14,000. A curve of static pressure loss versus mass flow rate for a square edge orifice with pipe taps of area equivalent to the flowmeter passage area is presented for comparison. Flowmeter static pressure loss is seen to increase rapidly with mass flow; however, the magnitude of this pressure loss, even at high mass flows, is not exceptionally great, and is considerably less than that for the equivalent area orifice.

V. CONCLUSIONS AND RECOMMENDATIONS

5.1 Conclusions. The practicability of a direct reading fluid flowmeter has been demonstrated and calibration curves for various values of RPM have been presented. A maximum error of 2% has been shown to exist in the results of three independent runs made for each of two values of RPM. The dependence of the flowmeter upon the velocity ratio U/V has been discussed and various plots presented for substantiation of this discussion. It is concluded, therefore, that a flowmeter of this type is capable of accurate and convenient measurement of fluid flow within the discussed limitations. Due to the critical nature of the flow within the meter it would be necessary, however, to calibrate each individual meter before practical employment.

5.2 Recommendations For Future Study. The tests made in this investigation were restricted by the limitations of the equipment used. In the theoretical derivation it has been shown that the mass flow reading is independent of the density of the fluid. The wooden construction of the flowmeter prevented pressurization and consequent density variation; thus, this theoretical property of

the meter has not been proven experimentally.

The question of power consumed by the rotation of the cylinder is another avenue not completely investigated. The meter required the total output of the 1/2 horsepower motor at 14,000 RPM for the maximum rate of mass flow studied. Detailed measurements of the torque, power required, etc. at various RPM and mass flows were not made.

The problem of head loss attributable to the meter has only partially been investigated. Velocity traverses ahead and after the flowmeter combined with the static pressure readings at these points would probably present a more complete aspect of the losses (if any) connected with a meter of this type.

The subject of optimum flowmeter dimensions is another possibility worthy of future investigation. In the meter studied the ratio of duct height to cylinder diameter was two. A greater value of this ratio would result in less obstruction to flow and less duct wall interference; however, restricting the duct size to practical limitations, this would mean a smaller cylinder diameter and require higher values of RPM to maintain the proper range of the velocity ratio U/V.

There is, then, a broad field of investigation ahead for perfection and complete explanation of this type of equipment.

BIBLIOGRAPHY

1. Tennant, S.M. and Turner, J.R.: A Flowmeter Designed To Measure Mass Flow By Direct Calibration, thesis, Massachusetts Institute of Technology, 1950.

2. Magnus, G.: Annalen Der Physik U. Chemie, 88, p. 1-14, 1853.

3. Lord Rayleigh: On The Irregular Flight Of A Tennis Ball, Scientific Papers I, p. 344-346, 1877.

4. Goldstein, S.: Modern Developments In Fluid Dynamics, Oxford University Press, 1943.

5. Lafay: Contribution Experimentale A L'Aerodynamique Du Cylindre, Rev. Mecanique, 30, 1912.

6. Thom, A.: Experiments On The Air Forces On Rotating Cylinders, R&M 1018, Aeronautical Research Committee, London, 1926.

7. Thom, A.: Experiments On The Flow Past A Rotating Cylinder, R&M 1410, Aeronautical Research Committee, London, 1931.

8. Thom, A.: The Pressure Round A Cylinder Rotating In An Air Current, R&M 1082, Aeronautical Research Committee, London, 1926.

9. Reid, E.G.: Tests Of Rotating Cylinders, NACA TN 209, 1925.

10. Durand, W.F.: Aerodynamic Theory, Vol. III, Julius Springer, Berlin, 1934.

11. Betz, A.: The "Magnus Effect", The Principle Of The Flettner Rotor, Translated as NACA TM 310, 1925.

12. Ahlborn, F.: The Magnus Effect In Theory And Reality, Translated as NACA TM 567, 1930.

13. Hildebrand, F.B.: Advanced Calculus For Engineers, Prentice Hall, New York, 1949.

14. Jeffreys and Jeffreys: Methods Of Mathematical Physics, Cambridge University Press, 1946.

15. Leary, W.A.: The Measurement Of Air Flow By Means Of The ASME Square-Edged Orifice With Flange Taps, Sloan Laboratory, M.I.T.,1949.

16. The Flettner Rotor Ship, Flight, Nov. 27, 1924, p. 741, London.

17. Testing The Flettner Rotor In Actual Flight, Flight, Dec. 4, 1924, p. 759, London.

18. Low, A.R.: The Reaction Of A Stream Of Viscous Fluid On A Rotating Cylinder, JRAS, Vol. XXIX, p. 100, London, 1925.

19. Prandtl, L.: The Generation Of Vortices In Fluids Of Small Viscosity, JRAS, Vol. XXXI, p. 720, London, 1927.

20. Relf, E.: Experiments On The Flow Behind A Rotating Cylinder In The Water Channel, R&M 1009, Aeronautical Research Committee, London, 1925.

21. Grose, P.C.: Magnus Effect Rotor Lift, Vertical Flight, General Publishing Co., Ohio, 1947.

22. Rizzo, F.: The Flettner Rotor Ship In The Light Of The Kutta-Joukowski Theory And Of Experimental Results, NACA TN 228, 1926.

23. Richardson, E.G.: Flow Of Air Adjacent To The Surface Of A Rotating Cylinder, R&M 1368, Aeronautical Research Committee, London, 1930.

24. Prandtl and Tietjens: Applied Hydro- And Aeromechanics, Mc Graw-Hill, New York, 1934.

25. ASME Power Test Code, Part 5, Chap. IV, American Society Of Mechanical Engineers, 1940.

26. Glauert, H.: Wind Tunnel Interference On Wings, Bodies, And Airscrews, R&M 1566, Aeronautical Committee, London, 1933.

GLOSSARY OF SYMBOLS

ΔP	pressure difference
M_a	air mass flow (lb./sec.)
ρ	air density
A	area
V	air stream velocity (ft./sec.)
Γ	circulation
R	cylinder radius
U	cylinder tangential speed (ft./sec.)
x	horizontal axis, imaginary plane
iy	vertical axis, imaginary plane
n	positive integer
k	duct height
F	potential function
z	complex variable
C	constant
w	stream velocity = dF/dz
g	gravitational constant
N	RPM (revolutions per minute)
R_e	Reynolds Number
d	cylinder diameter
μ	fluid viscosity
c	hydraulic diameter

q	dynamic pressure ($1/2\rho V^2$)	$lb./ft^2$
K	calibration coefficient ($\frac{Ma\ ACTUAL}{Ma\ THEO}$)	
T	temperature (degrees Rankine)	
P	pressure	
D_2	orifice diameter	
D_1	pipe diameter	
lbm	pounds mass	
sec	seconds	
primary	refers to pressure tap location (see Fig. 1)	
secondary	refers to pressure tap location (see Fig. 1)	

APPENDIX I

SAMPLE CALCULATIONS

The sample calculations which follow are for Line 1, Table 1, pages 47 and 48.

Column (1): P_1 orifice

P_1 orifice = P_1 gauge + P_{atm}

P_1 gauge from manometer = 0 (not shown in table)

P_{atm} = 29.85 in. hg. = 407 in. water

Column (2): ΔP orifice

ΔP orifice from manometer = .91 in. water

Column (3): T

Stream temperature used in computation of mass flow = 520°R.

Column (4): M_a actual

Mass flow computed from orifice data

a. From Fig. II-B, Appendix II, read K = .656 for ΔP orifice = .91 in. water

b. From Fig. II-A, Appendix II, read Y = 1.00 for $\frac{\Delta P \text{ orifice}}{P_1 \text{ orifice}} = \frac{.91}{407} = .0022$

c. Compute M_a from:

$$M_a = .1145 D_2^2 K Y \sqrt{\frac{P_1}{T} \Delta P_{ORIFICE}} \quad *$$

where D_2 = orifice diameter = 6.30 in.

P_1 = 29.85 in. hg.

T = 520 °R

$\Delta P_{orifice}$ = .91 in. water

$$M_a = (.1145)(6.3)^2(.656)(1.0)\sqrt{\frac{29.85}{520}(.91)} = .68$$

Column (5): V

$M_a = \rho AV$ $\qquad V = \frac{M_a}{\rho A} = \frac{.68}{(.002378)(\frac{64}{144})(32.2)} = 19.95$

A = flowmeter duct area = $\frac{64}{144}$ Ft^2

Column (6): q

$q = \frac{1}{2}\rho V^2 = \frac{1}{2}(.002378)(19.95)^2 = .474$

Column (7): $\Delta P_{flowmeter}$ (primary)

from draft gauge ΔP = .32 in. water

Column (8) N

N = RPM measured by strobotac = 3290 RPM

---

* W.A. Leary, Ref. 15, p. 9.

Column (9): U

$$U = \frac{2\pi RN}{60} = \frac{2\pi(1/6)(3290)}{60} = 57.4$$

where R = radius of cylinder = 1/6 ft.

Column (10): $\frac{\Delta P}{N} \times 10^4$ (primary)

$$\frac{.32}{3290} \times 10^4 = .974$$

Column (11): U/V

$$U/V = \frac{57.4}{19.95} = 2.88$$

Column (12): $\frac{\Delta P}{q}$

ΔP = .32 in. water = 1.67 lbs/ft^2

$$\frac{\Delta P}{q} = \frac{1.67}{.474} = 3.52$$

Column (13): K

K = calibration coefficient = $\frac{Ma\ ACTUAL}{Ma\ THEO}$

M_a actual = .68 lbm/sec

M_a theo. = $(.155)(\frac{\Delta P}{N} \times 10^4) = (.155)(.974)$

$$K = \frac{(.68)}{(.155)(.974)} = 4.51$$

Column (14): ΔP flowmeter (secondary)

from manometer ΔP = .51 in. water

Column (15): $\frac{\Delta P}{N} \times 10^4$ (secondary)

$$\frac{.51}{3290} \times 10^4 = 1.56$$

TABLE I

Flowmeter Data For 3300 RPM

20 March 1951 Barometer 29.85 "hg

(1) P_1 ABS ORIFICE "H_2O	(2) ΔP ORIFICE "H_2O	(3) T °R	(4) Ma ACTUAL LBM/SEC	(5) V FT/SEC	(6) γ LB/FT^2	(7) ΔP METER "H_2O PRIMARY	(8) N RPM
407	.91	520	.68	20.0	.47	.32	3290
407	.99	520	.71	20.7	.51	.32	3300
407	1.30	520	.82	23.9	.68	.39	3240
407	2.09	520	1.03	30.2	1.07	.50	3260
407	3.97	520	1.41	41.4	2.03	.51	3290
403	10.1	520	2.22	65.1	5.04	.17	3350
403	12.7	520	2.49	73.0	6.32	-.04	3280
403	13.9	520	2.60	76.3	6.91	-.20	3250
402	15.4	520	2.71	79.5	7.52	-.24	3325
401	17.1	520	2.86	83.9	8.38	-.39	3250
400	18.8	520	2.99	87.6	9.14	-.51	3210
400	20.3	520	3.10	91.0	9.87	-.51	3280
399	24.0	520	3.39	99.5	11.80	-.31	3250
398	27.9	523	3.60	106.8	13.32	.12	3280
398	32.2	524	3.86	113.3	15.35	.59	3280
397	36.5	525	4.08	121.0	17.35	.80	3280
396	41.2	525	4.30	127.2	19.28	1.18	3290
395	45.5	525	4.48	133.0	21.0	1.48	3315
393	51.4	525	4.75	140.7	23.6	1.53	3310
391	53.5	529	4.82	143.9	24.6	1.45	3340
391	59.5	530	5.05	151.0	27.1	1.51	3340
390	63.7	533	5.17	156.0	28.9	1.40	3350
390	68.5	534	5.35	161.2	30.9	1.38	3260
389	76.0	535	5.58	168.2	33.7	1.25	3330

TABLE I

(continued)

(9) U FT/SEC	(10) $\frac{\Delta P}{N} \times 10^4$ PRIMARY	(11) $\frac{U}{V}$	(12) $\frac{\Delta P}{\rho}$	(13) K	(14) ΔP METER "H_2O SECONDARY	(15) $\frac{\Delta P}{N} \times 10^4$ SECONDARY
57.4	.97	2.83	3.52	4.51	.51	1.56
57.6	.97	2.79	3.26	4.71	.51	1.55
56.5	1.21	2.36	2.90	4.34	.63	1.95
56.9	1.54	1.89	2.37	4.32	1.26	3.86
57.4	1.55	1.39	1.31	5.87	1.26	3.83
58.5	.51	.90	.18	28.1	1.03	3.08
57.2	-.12	.78	-.06	-134	.87	2.65
56.7	-.62	.75	-.15	-27.0	.79	2.42
58.0	-.72	.73	-.17	-24.3	.75	2.25
56.7	-1.20	.68	-.24	-15.4	.79	2.42
56.0	-1.59	.64	-.29	-12.1	.75	2.33
57.3	-1.56	.63	-.27	-12.8	.79	2.40
56.7	-.96	.57	-.14	-22.3	1.26	3.87
57.3	.37	.54	.05	62.8	2.13	6.50
57.3	1.80	.51	.20	13.8	2.48	7.57
57.3	2.44	.47	.24	10.8	2.44	7.45
57.4	3.59	.45	.32	7.32	2.01	6.12
57.3	4.47	.44	.37	6.46	2.01	6.06
57.6	4.62	.41	.34	6.63	1.69	5.10
58.3	4.35	.41	.31	7.15	1.66	4.95
58.3	4.52	.39	.29	7.21	1.73	5.20
58.5	4.18	.38	.25	7.96	1.70	5.04
56.9	4.23	.35	.23	8.15	1.73	5.32
58.1	3.76	.35	.19	9.59	1.66	4.97
57.6	3.61	.34	.18	10.15	1.50	4.54
57.3	3.42	.32	.16	11.00	1.73	5.28

TABLE II

Flowmeter Data For 4350 RPM

20 March 1951 Barometer 29.76 "hg

(1) P_1 ABS ORIFICE "H_2O	(2) ΔP ORIFICE "H_2O	(3) T °R	(4) Ma ACTUAL LBM/SEC	(5) V FT/SEC	(6) ρ LB/FT^2	(7) ΔP METER "H_2O PRIMARY	(8) N RPM
405	.99	536	.70	21.05	.53	.47	4350
405	1.10	535	.74	22.2	.59	.48	4350
405	1.46	534	.85	25.2	.76	.55	4350
405	2.36	534	1.08	32.3	1.24	.72	4350
405	3.23	534	1.26	37.7	1.69	.83	4370
404	4.80	533	1.52	45.7	2.49	.91	4350
404	7.80	530	1.95	58.3	4.04	.86	4350
401	12.25	530	2.41	72.2	6.19	.64	4350
400	14.30	530	2.60	77.9	7.21	.52	4350
400	15.50	530	2.70	80.9	7.80	.45	4330
400	17.30	530	2.85	85.3	8.68	.31	4280
398	18.85	530	2.96	88.7	9.35	.30	4330
398	20.6	530	3.10	92.9	10.23	.20	4350
397	22.3	530	3.20	95.9	10.95	.12	4330
397	24.1	530	3.33	99.8	11.90	.06	4330
397	28.2	530	3.59	107.5	13.8	.12	4370
396	32.4	530	3.83	114.5	15.6	.63	4340
396	36.7	530	4.06	121.5	17.6	1.21	4350
393	41.8	532	4.31	129.5	20.0	1.93	4450
393	45.5	532	4.45	133.5	21.2	2.28	4350
392	50.9	533	4.69	141.0	23.6	2.77	4360
392	56.7	534	4.91	147.5	25.8	2.98	4250
390	67.5	535	5.28	159.0	30.1	3.43	4400
389	79.2	535	5.67	171.0	34.8	3.73	4340
388	90.6	536	5.99	180.5	38.8	3.95	4400

TABLE II

(continued)

(9) U FT/SEC	(10) $\frac{\Delta P}{N} \times 10^4$ PRIMARY	(11) $\frac{U}{V}$	(12) $\frac{\Delta P}{g}$	(13) K	(14) ΔP METER "H_2O SECONDARY	(15) $\frac{\Delta P}{N} \times 10^4$ SECONDARY
75.8	1.08	3.60	4.63	4.17	.75	1.72
75.8	1.11	3.42	4.28	4.27	.75	1.72
75.8	1.27	2.97	3.79	4.32	.87	2.00
75.8	1.66	2.35	3.02	4.18	1.10	2.53
76.1	1.90	2.02	2.55	4.26	1.30	2.97
75.8	2.09	1.66	1.90	4.69	1.73	3.98
75.8	1.98	1.30	1.11	6.32	2.09	4.81
75.8	1.47	1.05	.54	10.55	1.97	4.53
75.8	1.20	.97	.38	13.95	1.85	4.26
75.5	1.04	.93	.30	16.7	1.77	4.09
74.5	.72	.88	.19	25.5	1.73	4.04
75.5	.69	.85	.17	27.6	1.73	3.99
75.8	.46	.82	.10	43.5	1.73	3.98
75.5	.28	.79	.06	73.7	1.77	4.09
75.5	.14	.76	.03	153	1.81	4.18
74.4	.28	.69	.05	82.7	2.09	4.90
75.6	1.46	.66	.21	16.9	2.99	6.90
75.8	2.73	.62	.35	9.42	3.07	7.07
77.5	4.24	.60	.51	6.55	3.35	7.53
75.8	5.25	.57	.56	5.47	2.64	6.08
76.0	6.35	.54	.61	4.77	2.44	5.59
74.1	7.02	.50	.60	4.51	2.48	5.84
76.7	7.80	.48	.59	4.37	2.09	4.75
75.6	8.59	.44	.56	4.25	1.97	4.54
76.7	8.97	.42	.53	4.31	1.54	3.50

TABLE III

Flowmeter Data For 6400 RPM

20 March 1951 Barometer 29.76 "hg

(1) P_1 ABS ORIFICE "H_2O	(2) ΔP ORIFICE "H_2O	(3) T °R	(4) Ma ACTUAL LBM/SEC	(5) V FT/SEC	(6) ρ LB/FT^2	(7) ΔP METER "H_2O PRIMARY	(8) N RPM
404	.95	535	.68	20.5	.50	.74	6400
404	1.38	533	.83	24.8	.73	.91	6400
404	2.24	531	1.05	31.5	1.18	1.09	6460
403	4.25	531	1.44	43.2	2.21	1.36	6400
403	6.93	531	1.83	54.9	3.53	1.73	6460
401	11.65	530	2.37	71.0	6.02	2.00	6400
401	14.4	530	2.62	78.5	7.32	2.04	6400
400	15.5	530	2.70	80.9	7.80	2.05	6400
399	17.45	530	2.86	85.7	8.50	2.00	6400
399	18.9	530	2.96	88.8	9.38	1.97	6400
398	20.5	530	3.04	91.1	9.87	1.96	6400
398	22.5	530	3.43	103	12.6	1.91	6440
397	24.1	530	3.44	103	12.6	1.86	6400
397	25.9	530	3.45	104	12.7	1.80	6400
396	28.6	530	3.61	108	13.9	1.80	6420
396	30.3	530	3.71	111	14.7	1.80	6420
396	32.4	530	3.83	115	15.7	1.83	6420
394	37.3	531	4.08	122	17.7	1.99	6400
393	41.3	531	4.27	128	19.5	2.44	6430
393	46.1	532	4.40	132	20.7	3.30	6400
391	51.3	533	4.71	141	23.7	4.08	6400
390	62.1	535	5.13	154	28.2	4.90	6400
389	74.0	535	5.51	165	32.5	5.40	6400
388	85.1	535	5.83	175	36.3	5.95	6460

TABLE III

(continued)

(9) U FT/SEC	(10) $\frac{\Delta P}{N} \times 10^4$ PRIMARY	(11) $\frac{U}{V}$	(12) $\frac{\Delta P}{q}$	(13) K	(14) ΔP METER "H_2O SECONDARY	(15) $\frac{\Delta P}{N} \times 10^4$ SECONDARY
111.5	1.16	5.4[illegible]	7.70	3.81	1.38	2.16
111.5	1.42	4.49	6.45	3.75	1.58	2.48
113	1.69	3.59	4.80	4.02	1.70	2.63
111.5	2.12	2.58	3.20	4.39	1.89	2.96
112.8	2.68	2.06	2.52	4.40	2.33	3.61
111.5	3.12	1.57	1.73	4.90	3.04	4.76
111.5	3.19	1.42	1.45	5.30	4.22	6.60
111.5	3.21	1.38	1.37	5.42	4.42	6.91
111.5	3.13	1.30	1.27	5.71	4.45	6.97
111.5	3.08	1.26	1.09	6.20	4.57	7.15
111.5	3.06	1.23	1.03	6.40	4.62	7.22
112.2	2.97	1.09	.79	7.45	4.62	7.18
111.5	2.91	1.08	.77	7.62	4.62	7.22
111.5	2.81	1.08	.74	7.91	4.62	7.22
112	2.80	1.04	.67	8.32	4.73	7.36
112	2.80	1.01	.64	8.55	4.77	7.43
112	2.86	.98	.61	8.63	4.85	7.56
111.5	3.11	.91	.58	8.46	5.20	8.13
112.1	3.79	.88	.65	7.26	5.60	8.72
111.5	5.15	.85	.83	5.51	5.44	8.50
111.5	6.38	.79	.90	4.77	3.75	5.87
111.5	7.65	.73	.91	4.33	3.31	5.18
111.5	8.45	.68	.87	4.21	2.84	4.44
112.3	9.22	.65	.85	4.08	2.44	3.78

TABLE IV

Flowmeter Data For 8700 RPM

20 March 1951 Barometer 29.78 "hg

(1) P_1 ABS ORIFICE "H_2O	(2) ΔP ORIFICE "H_2O	(3) T °R	(4) Ma ACTUAL LBM/SEC	(5) V FT/SEC	(6) ρ LB/FT^2	(7) ΔP METER "H_2O PRIMARY	(8) N RPM
404	.67	535	.58	17.3	.36	.87	8700
404	1.34	535	.82	24.3	.70	1.15	8700
404	2.13	533	1.02	30.7	1.12	1.51	8750
404	3.86	533	1.37	41.1	2.00	1.83	8670
404	6.30	531	1.75	52.3	3.24	2.13	8670
403	10.8	530	2.27	68.0	5.49	2.72	8700
401	14.0	530	2.58	77.3	7.11	3.15	8700
400	15.6	530	2.70	80.9	7.79	3.35	8700
400	18.8	530	2.96	88.6	9.34	3.60	8740
399	22.3	530	3.21	96.1	11.0	3.80	8700
397	26.0	530	3.45	103.5	12.7	3.90	8670
397	30.3	530	3.72	111.5	14.8	4.05	8730
396	34.3	530	3.94	118.0	16.6	4.13	8740
395	38.6	530	4.15	124.4	18.5	4.25	8750
393	43.3	531	4.36	130.8	20.3	4.40	8710
392	48.2	533	4.57	137.0	22.3	4.75	8690
390	53.6	534	4.80	144	24.6	5.45	8790
389	57.8	535	4.95	149	26.3	5.80	8800
389	63.7	535	5.17	155	28.6	6.35	8700
389	69.2	535	5.33	160	30.4	6.75	8730
388	75.5	535	5.52	165	32.4	7.10	8700
385	80.7	535	5.68	170	34.5	7.35	8730

TABLE IV

(continued)

(9) U FT/SEC	(10) $\frac{\Delta P}{N} \times 10^4$ PRIMARY	(11) $\frac{U}{V}$	(12) $\frac{\Delta P}{g}$	(13) K	(14) ΔP METER "H_2O SECONDARY	(15) $\frac{\Delta P}{N} \times 10^4$ SECONDARY
151.8	1.00	8.78	12.80	3.72	1.66	1.91
151.8	1.32	6.25	8.53	3.97	2.17	2.49
152.5	1.73	4.97	7.00	3.80	2.56	2.93
151.3	2.11	3.68	4.75	4.18	2.64	3.04
151.3	2.46	2.90	3.43	4.58	2.88	3.32
151.8	3.13	2.23	2.58	4.67	3.27	3.75
151.8	3.62	1.96	2.31	4.59	3.66	4.21
151.8	3.85	1.88	2.24	4.52	3.86	4.44
152.4	4.12	1.72	2.00	4.64	4.26	4.88
151.8	4.37	1.58	1.80	4.74	4.81	5.52
151.3	4.50	1.46	1.60	4.94	5.28	6.09
152.4	4.64	1.37	1.43	5.17	6.50	7.44
152.4	4.73	1.29	1.30	5.36	8.00	9.15
152.5	4.86	1.23	1.20	5.50	7.96	9.10
152.0	5.05	1.16	1.13	5.56	7.68	8.80
151.7	5.47	1.11	1.11	5.38	7.10	8.18
153.2	6.22	1.07	1.15	4.98	5.99	6.82
150.0	6.76	1.01	1.15	4.72	4.88	5.68
151.8	7.30	.98	1.16	4.57	4.81	5.53
152.4	7.73	.95	1.16	4.45	4.53	5.19
151.8	8.17	.92	1.14	4.35	4.06	4.66
152.4	8.42	.90	1.11	4.35	3.55	4.08

TABLE V

Flowmeter Data For 10000 RPM

22 March 1951 Barometer 29.76 "hg

(1) P_1 ABS ORIFICE "H_2O	(2) ΔP ORIFICE "H_2O	(3) T °R	(4) Ma ACTUAL LBM/SEC	(5) V FT/SEC	(6) ρ LB/FT^2	(7) ΔP METER "H_2O PRIMARY	(8) N RPM
404	.75	520	.62	18.1	.39	.77	10000
404	1.10	520	.75	21.9	.57	1.06	10000
404	1.81	521	.95	27.9	.93	1.57	10000
404	3.50	521	1.29	37.8	1.70	2.13	10000
402	5.60	522	1.66	48.8	2.83	2.37	10000
402	9.40	522	2.14	63.0	4.72	2.90	9970
401	11.8	523	2.38	70.0	5.83-	3.25	10000
400	14.8	523	2.66	78.2	7.26	3.60	10000
398	17.8	524	2.90	85.7	8.72	4.03	10000
397	21.2	524	3.15	93.1	10.32	4.50	10000
397	23.2	524	3.30	97.5	11.3	4.70	10000
397	24.9	525	3.41	101	12.13	4.94	10000
396	26.8	525	3.52	104	12.85	5.10	10000
396	28.9	525	3.66	108.5	14.05	5.30	10040
394	31.0	526	3.77	112	14.92	5.40	10000
394	33.2	526	3.87	115	15.7	5.54	10000
394	35.5	527	4.03	119.5	17.2	5.60	10000
393	37.7	527	4.12	122	17.7	5.75	10000
393	39.6	528	4.20	125	18.6	5.85	10000
391	42.3	529	4.33	129	19.8	5.95	10000
390	44.5	529	4.40	131	20.5	6.15	10050
390	46.5	530	4.52	135	21.6	6.30	10000
389	49.2	530	4.61	138	22.6	6.43	10000
389	51.6	530	4.71	141	23.7	6.70	10000
389	56.7	532	4.92	148	26.1	7.10	10000
388	62.2	533	5.08	153	27.8	7.55	10000
386	67.0	534	5.27	159	30.1	8.05	10000
385	73.3	535	5.45	165	32.1	8.40	10000
383	78.4	536	5.58	169	33.8	8.80	10000
383	84.6	536	5.77	174	36.1	9.15	10000

TABLE V

(continued)

(9) U FT/SEC	(10) $\frac{\Delta P}{N} \times 10^4$ PRIMARY	(11) $\frac{U}{V}$	(12) $\frac{\Delta P}{q}$	(13) K	(14) ΔP METER "H_2O SECONDARY	(15) $\frac{\Delta P}{N} \times 10^4$ SECONDARY
174.5	.77	9.60	10.28	5.25	1.62	1.62
174.5	1.06	7.92	9.66	4.55	2.08	2.08
174.5	1.57	6.22	8.80	3.91	2.92	2.92
174.5	2.13	4.59	6.52	3.91	3.30	3.30
174.5	2.37	3.56	4.35	4.52	3.34	3.34
174	2.91	2.76	3.19	4.74	3.65	3.67
174.5	3.23	2.47	2.90	4.72	3.82	3.82
174.5	3.60	2.21	2.58	4.76	4.05	4.05
174.5	4.03	2.02	2.41	4.64	4.41	4.41
174.5	4.50	1.86	2.27	4.51	4.76	4.76
174.5	4.70	1.77	2.16	4.53	5.20	5.20
174.5	4.94	1.71	2.12	4.55	5.28	5.28
174.5	5.10	1.66	2.06	4.45	5.75	5.75
175	5.28	1.61	1.97	4.46	6.06	6.04
174.5	5.40	1.55	1.88	4.50	6.37	6.37
174.5	5.54	1.50	1.84	4.51	6.54	6.54
174.5	5.60	1.46	1.70	4.55	6.77	6.77
174.5	5.75	1.43	1.69	4.62	7.05	7.05
174.5	5.85	1.40	1.64	4.63	7.20	7.20
174.5	5.95	1.35	1.57	4.69	7.20	7.20
175	6.12	1.34	1.56	4.64	7.28	7.25
174.5	6.30	1.29	1.52	4.62	7.60	7.60
174.5	6.43	1.27	1.48	4.62	7.36	7.36
174.5	6.70	1.24	1.47	4.54	6.90	6.90
174.5	7.10	1.18	1.42	4.46	6.54	6.54
174.5	7.55	1.14	1.41	4.34	6.18	6.18
174.5	8.05	1.10	1.39	4.17	6.03	6.03
174.5	8.40	1.06	1.36	4.18	5.86	5.86
174.5	8.80	1.04	1.35	4.09	5.08	5.08
174.5	9.15	1.00	1.32	4.07	4.73	4.73

TABLE VI

Flowmeter Data For 12000 RPM

19 March 1951 Barometer 30.57 "hg

(1) P_1 ABS ORIFICE "H_2O	(2) ΔP ORIFICE "H_2O	(3) T °R	(4) Ma ACTUAL LBM/SEC	(5) V FT/SEC	(6) ρ LB/FT^2	(7) ΔP METER "H_2O PRIMARY	(8) N RPM
401	.79	518	.63	18.5	.41	.85	12100
401	.87	520	.66	19.4	.45	.91	12060
401	1.22	522	.76	22.1	.58	1.19	12040
401	2.01	522	1.00	29.3	1.02	1.82	12050
400	3.78	522	1.37	40.2	1.93	2.66	12060
400	10.45	522	2.26	66.3	5.24	3.50	12060
399	12,60	522	2.46	72.1	6.18	3.82	12070
397	14.30	522	2.62	76.8	7.02	4.05	12000
397	15.6	522	2.76	80.9	7.75	4.32	12100
408	16.85	522	2.88	84.5	8.47	4.50	12040
408	19.80	523	3.10	90.9	9.81	4.86	12050
412	23.80	524	3.40	100.5	12.25	5.45	12050
413	28.0	524	3.67	108.5	14.02	6.00	12000
420	32.8	525	3.99	118	16.53	6.75	12000
420	37.9	527	4.03	121.5	17.6	7.45	12070
420	42.9	528	4.53	135	21.7	8.07	12100
419	47.3	528	4.72	141	23.6	8.60	12050
418	53.0	529	4.97	148	26.1	9.30	12100
418	58.4	530	5.18	154	28.2	9.95	12100
417	64.2	530	5.40	161	30.8	10.48	12040
417	70.0	532	5.58	167	33.1	11.15	12040
418	76.0	535	5.80	175	36.4	11.75	12050
418	83.0	535	6.02	182	39.4	12.50	12050
419	89.0	535	6.23	188	42.2	12.90	12040

TABLE VI

(continued)

(9) U FT/SEC	(10) $\frac{\Delta P}{N} \times 10^4$ PRIMARY	(11) $\frac{U}{V}$	(12) $\frac{\Delta P}{g}$	(13) K	(14) ΔP METER "H_2O SECONDARY	(15) $\frac{\Delta P}{N} \times 10^4$ SECONDARY
212.5	.70	11.50	10.85	5.83	1.85	1.52
210.5	.76	10.85	10.55	5.65	1.93	1.60
210	.98	9.50	10.62	4.93	2.40	1.99
210	1.51	7.18	9.25	4.27	3.42	2.84
210.5	2.21	5.24	7.18	4.00	4.60	3.81
210.5	2.91	3.18	3.47	5.01	4.60	3.81
210.5	3.17	2.92	3.21	5.01	4.80	3.98
209.5	3.38	2.73	3.00	5.00	4.92	4.10
211	3.57	2.61	2.89	4.98	5.00	4.13
210	3.74	2.49	2.76	4.97	4.96	4.12
210	4.03	2.31	2.58	4.97	5.31	4.40
210	4.52	2.09	2.31	4.86	5.59	4.64
209.5	5.00	1.93	2.22	4.73	5.98	4.99
209.5	5.62	1.77	2.12	4.58	6.38	5.32
210.5	6.18	1.73	2.20	4.26	7.00	5.81
211	6.67	1.56	1.94	4.37	7.55	6.24
210	7.13	1.50	1.90	4.27	8.26	6.85
211	7.69	1.43	1.85	4.17	8.77	7.25
211	8.23	1.37	1.80	4.06	9.32	7.70
210	8.70	1.31	1.77	4.00	9.68	8.03
210	9.25	1.26	1.75	3.89	10.30	8.55
210	9.75	1.20	1.68	3.84	10.00	8.30
210	10.38	1.16	1.65	3.74	9.93	8.25
210	10.70	1.12	1.59	3.75	9.55	7.92

TABLE VII

Flowmeter Data For 12000 RPM

22 March 1951 Barometer 29.78 "hg

(1) P_1 ABS ORIFICE "H_2O	(2) ΔP ORIFICE "H_2O	(3) T °R	(4) Ma ACTUAL LBM/SEC	(5) ΔP METER "H_2O PRIMARY	(6) N RPM	(7) $\frac{\Delta P}{N} \times 10^4$ PRIMARY
405	.91	534	.68	.97	12020	.81
405	1.26	534	.79	1.28	12000	1.07
404	2.00	534	.97	1.91	12000	1.59
404	3.86	534	1.37	2.75	12030	2.29
404	5.60	533	1.65	3.07	12000	2.56
403	9.55	532	2.14	3.50	12000	2.92
402	13.6	531	2.54	4.10	12000	3.42
400	16.3	531	2.81	4.47	12000	3.72
398	19.6	530	3.02	4.85	12000	4.04
397	23.2	530	3.27	5.33	12000	4.44
396	26.9	530	3.49	5.83	12000	4.87
394	31.0	531	3.74	6.40	12000	5.33
394	35.2	532	3.98	6.90	12000	5.75
393	39.5	532	4.17	7.45	12000	6.21
392	44.5	532	4.42	8.00	12000	6.67
390	48.2	533	4.55	8.50	12000	7.08
389	54.5	533	4.80	9.00	12000	7.50
388	58.8	534	4.97	9.45	12000	7.87
386	64.8	535	5.18	9.90	12000	8.25
385	70.0	536	5.32	10.33	12000	8.62
385	76.5	537	5.53	10.80	12000	9.00
382	81.5	538	5.68	11.15	12000	9.30
382	86.5	540	5.78	11.60	12000	9.67

TABLE VIII

Flowmeter Data For 12000 RPM

15 March 1951 Barometer 29.67 "hg

(1) P_1 ABS ORIFICE "H_2O	(2) ΔP ORIFICE "H_2O	(3) T °R	(4) Ma ACTUAL LBM/SEC	(5) ΔP METER "H_2O PRIMARY	(6) N RPM	(7) $\frac{\Delta P}{N} \times 10^4$ PRIMARY
382	.75	524	.60	.71	12000	.59
382	.83	524	.63	.77	12100	.64
382	1.06	523	.71	1.01	12070	.85
382	1.77	522	.92	1.61	12080	1.34
382	3.46	522	1.28	2.45	12010	2.04
381	3.63	522	1.99	3.19	12100	2.64
380	11.4	522	2.28	3.52	12050	2.92
378	13.8	522	2.50	3.86	12080	3.20
377	17.1	522	2.77	4.25	12050	3.53
377	20.1	522	3.00	4.60	12010	3.83
375	23.5	522	3.22	5.06	12100	4.19
373	27.4	524	3.46	5.53	12020	4.60
373	31.3	524	3.67	6.00	12020	4.98
372	35.6	525	3.90	6.50	12040	5.39
371	39.6	526	4.10	7.00	12050	5.80
370	44.0	528	4.26	7.38	12070	6.12
368	48.8	528	4.46	7.78	12100	6.44
367	53.0	530	4.63	7.96	12000	6.63
366	58.9	530	4.83	8.54	12190	7.00
366	63.2	531	4.98	8.65	12100	7.15
364	68.5	533	5.13	8.93	12000	7.45
363	74.5	535	5.37	9.26	12100	7.66
362	79.8	535	5.53	9.55	12000	7.96
360	84.0	537	5.55	9.88	12100	8.16
359	90.0	540	5.67	10.13	12000	8.46
358	95.3	542	5.79	10.50	12060	8.71
358	100.0	543	5.88	10.60	12060	8.82
356	105.5	546	5.99	10.90	12090	9.02
355	110.0	550	6.07	10.90	12040	9.04
354	114.5	552	6.13	11.25	12150	9.26
354	120.0	555	6.25	11.05	12000	9.22
350	123.0	542	6.32	11.35	12050	9.42
349	128.0	535	6.44	11.85	12050	9.83

TABLE IX

Flowmeter Data For 14000 RPM

22 March 1951 Barometer 29.78 " hg

(1) P_1 ABS ORIFICE "H_2O	(2) ΔP ORIFICE "H_2O	(3) T °R	(4) Ma ACTUAL LBM/SEC	(5) V FT/SEC	(6) ρ LB/FT^2	(7) ΔP METER "H_2O PRIMARY	(8) N RPM
405	.87	539	.66	19.9	.47	1.08	14000
405	1.26	538	.79	24.0	.68	1.37	14040
404	1.97	536	.98	29.6	1.04	1.99	14000
404	3.78	535	1.36	41.2	2.02	3.23	14000
403	5.95	535	1.69	51.1	3.09	3.83	14000
403	10.1	534	2.20	66.2	5.21	4.30	14000
400	13.7	534	2.48	74.6	6.62	4.68	14000
398	16.3	533	2.76	83.0	8.20	5.10	14000
398	19.4	533	3.00	90.2	9.63	5.55	14000
397	22.9	534	3.24	97.5	11.3	5.98	14000
396	26.8	534	3.48	104.8	13.1	6.50	14000
394	30.8	534	3.71	111.7	14.8	7.00	14000
393	34.7	534	3.93	118.4	16.7	7.50	14000
391	39.4	534	4.17	125.5	18.7	8.13	14000
390	44.5	535	4.40	133.0	20.9	8.70	14000
389	49.2	535	4.58	138.5	22.8	9.40	14000
389	53.6	536	4.78	144.5	24.9	9.90	14000
388	58.8	537	4.97	151.0	27.1	10.58	14000
386	64.2	537	5.15	156.5	29.2	11.10	14000
385	70.1	538	5.32	161.5	30.9	11.70	14000
384	75.5	539	5.50	167.0	33.2	12.25	14000
382	80.3	541	5.60	171.3	35.0	12.90	14000
382	85.8	542	5.76	176.2	36.9	13.50	14000

TABLE IX

(continued)

(9) U FT/SEC	(10) $\frac{\Delta P}{N} \times 10^4$ PRIMARY	(11) $\frac{U}{V}$	(12) $\frac{\Delta P}{g}$	(13) K	(14) ΔP METER "H_2O SECONDARY	(15) $\frac{\Delta P}{N} \times 10^4$ SECONDARY
244	.77	12.25	11.82	5.50	2.21	1.58
245	.98	10.22	10.45	5.18	2.87	2.05
244	1.42	8.25	9.95	4.46	3.74	2.67
244	2.30	5.93	8.31	3.82	5.79	4.13
244	2.73	4.78	6.45	3.99	6.10	4.35
244	3.07	3.69	4.29	4.42	6.03	4.30
244	3.35	3.27	3.68	4.78	5.98	4.27
244	3.64	2.94	3.24	4.89	6.10	4.35
244	3.96	2.71	3.10	4.89	6.22	4.44
244	4.27	2.50	2.74	4.89	6.50	4.64
244	4.64	2.33	2.58	4.84	6.62	4.72
244	5.00	2.19	2.46	4.79	7.01	5.00
244	5.35	2.06	2.34	4.74	7.21	5.15
244	5.80	1.95	2.26	4.64	7.60	5.43
244	6.20	1.84	2.16	4.58	7.80	5.57
244	6.72	1.76	2.14	4.40	8.35	5.96
244	7.07	1.69	2.06	4.37	8.90	6.35
244	7.55	1.62	2.03	4.25	9.34	6.66
244	7.93	1.56	1.98	4.19	10.12	7.21
244	8.35	1.51	1.97	4.11	10.35	7.40
244	8.75	1.46	1.92	4.06	10.90	7.78
244	9.22	1.42	1.92	3.92	11.15	7.97
244	9.65	1.39	1.90	3.85	11.58	8.26

TABLE X

Flowmeter Data For 14000 RPM

8 March 1951 Barometer 29.78 "hg

(1) P_1 ABS ORIFICE "H_2O	(2) ΔP ORIFICE "H_2O	(3) T °R	(4) Ma ACTUAL LBM/SEC	(5) ΔP METER "H_2O PRIMARY	(6) N RPM	(7) $\frac{\Delta P}{N} \times 10^4$ PRIMARY
381	11.95	518	2.35	4.43	13800	3.21
381	14.70	518	2.43	4.80	13800	3.48
381	17.80	520	2.84	5.35	14240	3.76
379	21.00	520	3.03	5.85	14100	4.15
378	24.30	521	3.29	6.20	14100	4.39
376	28.90	524	3.56	6.75	14000	4.82
375	33.00	524	3.78	7.30	14000	5.21
372	36.00	530	3.90	7.75	14150	5.48
372	41.80	530	4.18	8.46	14100	6.00
371	44.90	530	4.31	8.94	14050	6.36
370	50.80	531	4.55	9.52	13950	6.82
368	56.40	533	4.58	10.15	14000	7.24
367	60.90	533	4.92	10.70	14000	7.65
366	66.00	534	5.05	11.30	14000	8.08
365	72.00	535	5.28	11.88	13950	8.50
364	77.10	535	5.40	12.68	14180	8.94
362	81.90	537	5.50	13.14	14180	9.29
360	88.00	540	5.65	13.78	14120	9.74
359	93.50	541	5.78	14.10	14120	9.98

TABLE XI

Flowmeter Data For 14000 RPM

13 March 1951 Barometer 30.26 "hg

(1) P_1 ABS ORIFICE "H_2O	(2) ΔP ORIFICE "H_2O	(3) T °R	(4) Ma ACTUAL LBM/SEC	(5) ΔP METER "H_2O PRIMARY	(6) N RPM	(7) $\frac{\Delta P}{N} \times 10^4$ PRIMARY
385	.63	520	.55	.92	14130	.65
386	.71	520	.59	.96	14130	.68
386	.98	520	.69	1.18	14150	.83
385	1.65	520	.89	1.69	14250	1.19
385	3.19	521	1.23	2.84	14340	1.98
385	8.40	521	1.99	4.10	14150	2.90
383	11.3	521	2.29	4.28	14050	3.05
381	14.3	521	2.55	4.70	14300	3.29
381	17.5	521	2.81	5.15	14100	3.65
380	20.5	521	3.04	5.55	14130	3.92
379	23.9	522	3.26	5.95	14130	4.20
378	27.8	522	3.51	6.40	14000	4.57
378	31.9	524	3.74	7.00	14150	4.95
376	31.9	525	3.71	6.95	14250	4.88
375	36.5	527	3.96	7.50	14130	5.30
375	36.4	527	3.96	7.50	14180	5.30
374	39.6	528	4.10	8.00	14130	5.65
373	45.0	530	4.33	8.60	14160	6.08
371	49.2	530	4.48	9.08	14050	6.46
371	54.8	531	4.72	9.65	14080	6.86
371	54.3	531	4.70	9.65	14130	6.82
368	58.8	534	4.71	10.00	14000	7.15
367	64.2	535	5.02	10.75	14430	7.45
367	69.1	536	5.21	11.08	14180	7.81
366	73.7	543	5.26	11.50	14240	8.08

TABLE XII

Static Pressure Loss For 14000 RPM

27 February 1951 Barometer 29.65 "hg

(1) P_1 ABS ORIFICE "H_2O	(2) ΔP ORIFICE "H_2O	(3) T °R	(4) Ma ACTUAL LBM/SEC	(5) ΔP_{loss} "H_2O
384	.71	505	.59	.32
384	1.18	505	.77	.32
384	1.18	505	.77	.39
385	1.26	505	.79	.39
385	1.62	505	.90	.39
385	2.64	505	1.14	.47
385	4.77	505	1.53	.63
385	11.81	510	2.37	.99
384	17.95	520	2.88	1.81
379	20.2	520	2.91	2.40
379	22.9	520	3.21	2.48
378	24.0	520	3.27	2.68
377	24.6	522	3.30	2.99
377	24.5	523	3.42	2.99
377	28.1	523	3.51	3.15
376	29.6	525	3.59	3.43
376	32.5	525	3.75	3.54
375	33.5	526	3.80	3.96
374	35.4	526	3.89	3.96
374	36.4	528	3.92	4.18
373	39.1	528	4.07	4.33
372	40.7	530	4.13	4.53
372	42.8	530	4.20	4.92
372	44.4	532	4.28	5.23
370	48.2	534	4.42	5.52
370	48.7	534	4.46	5.60
368	50.9	535	4.53	6.10
367	51.4	535	4.53	6.22
367	54.6	536	4.66	6.38
367	57.3	537	4.76	6.73
367	61.6	539	4.89	7.28
366	65.3	540	5.00	7.76
364	69.2	540	5.13	8.20

APPENDIX II

ORIFICE DATA

Actual mass rate of flow for use as a standard by which to judge the flowmeter is computed from the following equation: *

$$Ma = .1145\ D_2^2 K Y \sqrt{\frac{P_1}{T} \Delta P_{ORIFICE}} \qquad \text{(II-1)}$$

where M_a = mass rate of flow, lbm/sec

D_2 = orifice diameter = 6.30 inches

K = flow coefficient, dimensionless

Y = expansion factor, dimensionless

P_1 = static pressure before orifice, in. hg. abs.

T = temperature before orifice, $^{\circ}$R

ΔP orifice = pressure drop across orifice, in. water

P_1, T, and ΔP orifice are measured quantities recorded for each run at each mass flow increment.

Y, the expansion factor, is determined from Fig. II-A which is a plot of the relation #

$$Y = 1 - \left[.41 + .35\left(\frac{D_2}{D_1}\right)^4\right]\left[\frac{\Delta P_{ORIFICE}}{P_1 k}\right] \qquad \text{(II-2)}$$

---

* Leary, Ref. 15, p. 9, Eq.8.

\# Leary, Ref. 15, p. 5, Eq.4.

which, with constant diameter ratio, $\frac{D_2}{D_1}$, and constant ratio of specific heats, k, becomes a linear function of $\frac{\Delta P_{ORIFICE}}{P_1}$. Therefore, with a value of $\frac{\Delta P_{ORIFICE}}{P_1}$ computed from measured quantities, Y may be read from Fig. II-A.

K, the flow coefficient, has been experimentally determined by the ASME for this type of orifice and has been plotted versus Reynolds Number for specific values of $\frac{D_2}{D_1}$ * . Use of a plot such as this would require a trial and error computation of K since the mass flow cannot be found until K is known and K cannot be found until the Reynolds Number, which is a function of mass flow, is known.

To eliminate the necessity for a trial and error solution for K, two assumptions have been made:

(a) P_1 assumed constant = 29.9 in. hg. = 407 in water

(b) T assumed constant = 530 °R

With these assumptions Y becomes a function of $\Delta P_{orifice}$ only and equation (II-2) becomes

$$Y = 1 - .000798\,\Delta P_{ORIFICE} \qquad \text{(II-3)}$$

---

* Ref. 25, Fig. 34f

Substituting this relation for Y into equation (II-1) we obtain

$$M_a = (.1145)(6.3)^2(K)(1-.000798\Delta P_{ORIFICE})\sqrt{\frac{29.9}{530}}\sqrt{\Delta P_{ORIFICE}}$$

which reduces to

$$M_a = 1.08K(1-.000798\,\Delta P_{ORIFICE})\sqrt{\Delta P_{ORIFICE}} \qquad \text{(II-4)}$$

The Reynolds Number based on the orifice diameter is given by *

$$R_e = \frac{15.28\,M_a}{D_2\,\mu} \qquad \text{(II-5)}$$

Substituting equation (II-4) and taking μ, the viscosity = .000012 lb/ft-sec, the expression for Reynolds Number becomes

$$R_e = (2.16\times10^5)K(1-.000798\Delta P_{ORIFICE})\sqrt{\Delta P_{ORIFICE}} \qquad \text{(II-6)}$$

For a direct method of finding K, a curve of K versus $\Delta P_{orifice}$ would be desirable. Therefore, we proceed as follows:

(a) For an assumed value of $\Delta P_{orifice}$, assume a K and compute R_e from equation II-6.

(b) Read K for computed R_e from Fig. 34f of Ref.

---

* Leary, Ref. 15, p. 12, Eq. 10b

25 and use as new assumed K for repeat of step (a).

(c) Plot K versus $\Delta P_{orifice}$ for various assumed values of $\Delta P_{orifice}$. This plot will be a direct means for determining K, the flow coefficient.

Figure II-B is the result of the above procedure. Test calculations using Fig. 34f of Ref. 25 exclusively show that, for the range of pressures and temperatures investigated, there is negligible error introduced by assuming a constant P_1 and T for the purpose of determining K.

With Y and K thus determined from Figs. II-A and II-B, actual mass rate of flow is computed from equation (II-1).

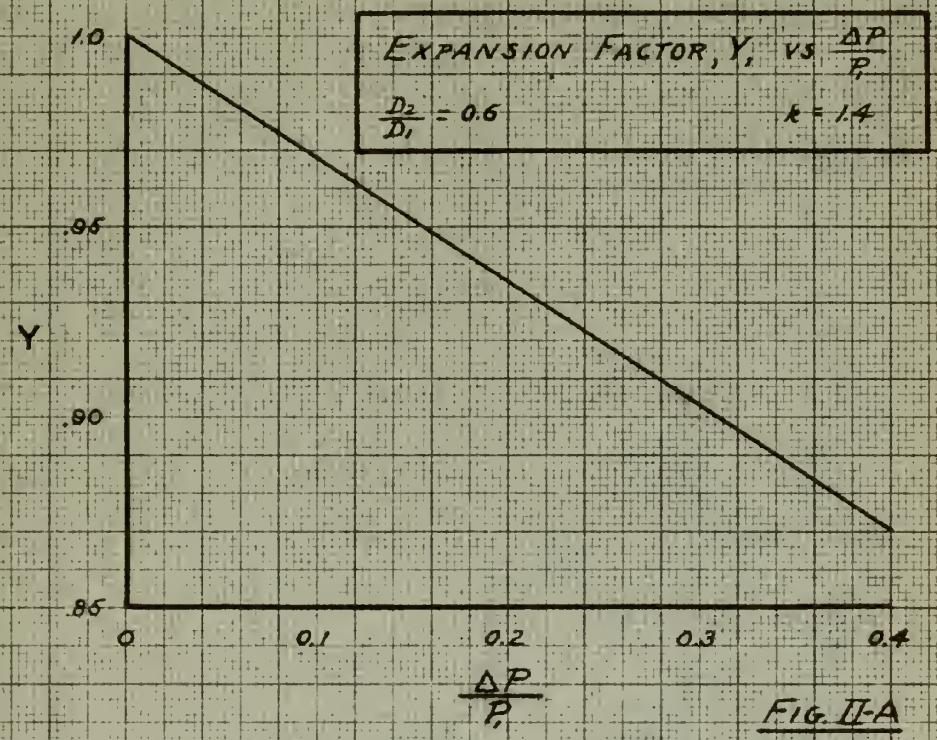

FIG. II-A

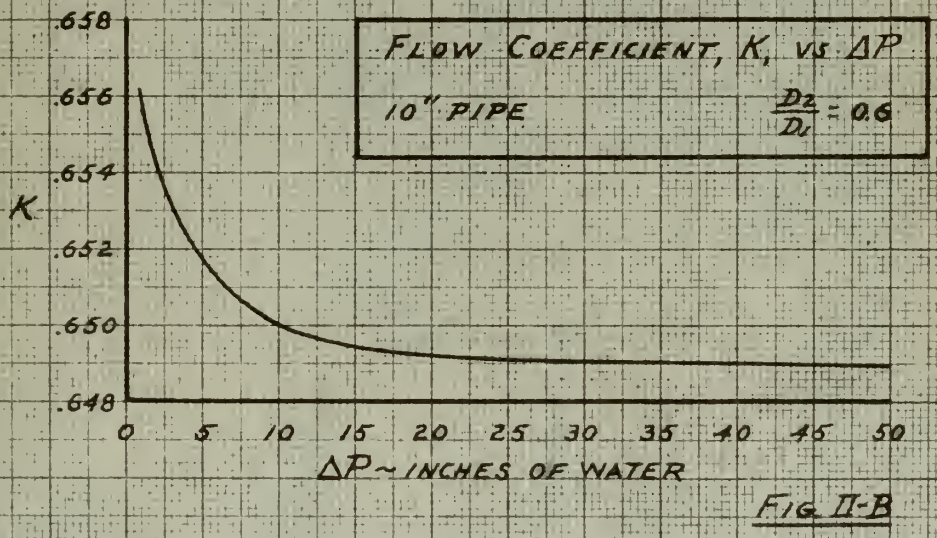

FIG. II-B

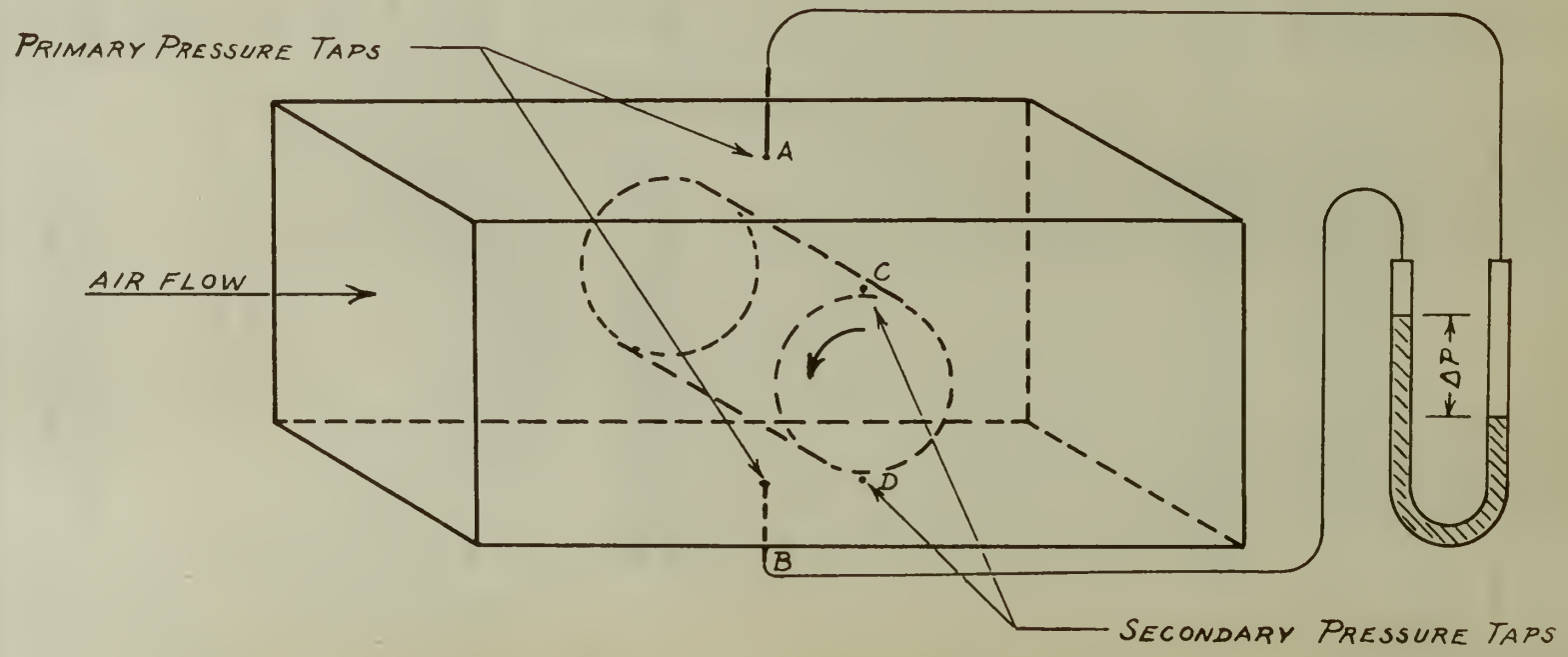

SCHEMATIC SKETCH OF FLOWMETER

FIG. 1

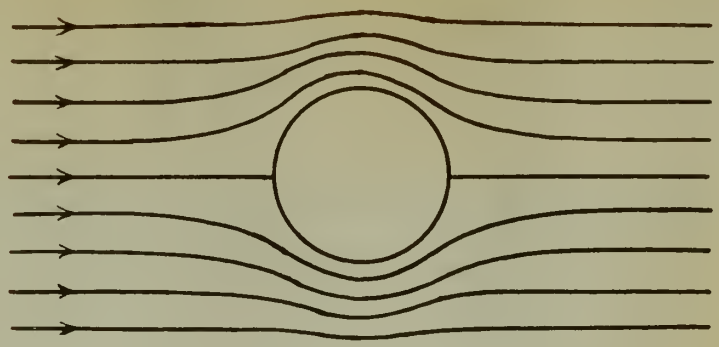

Fig. 2a Uniform Potential Flow Around A Circular Cylinder

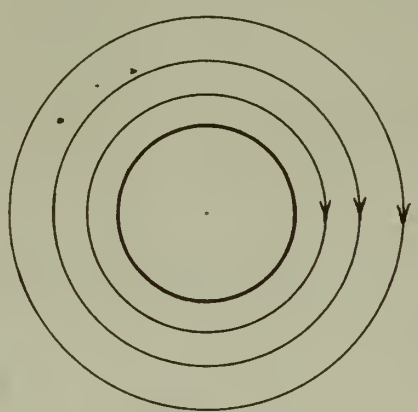

Fig. 2b Potential Vortex Flow With Cylinder As Core

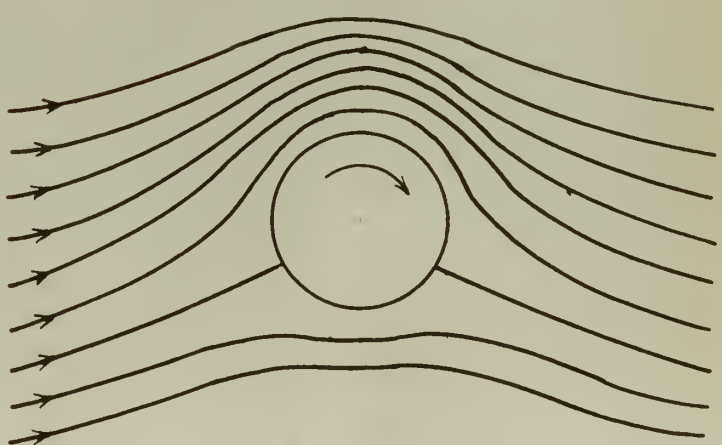

Fig. 2c Superposition Of Two Preceding Flows

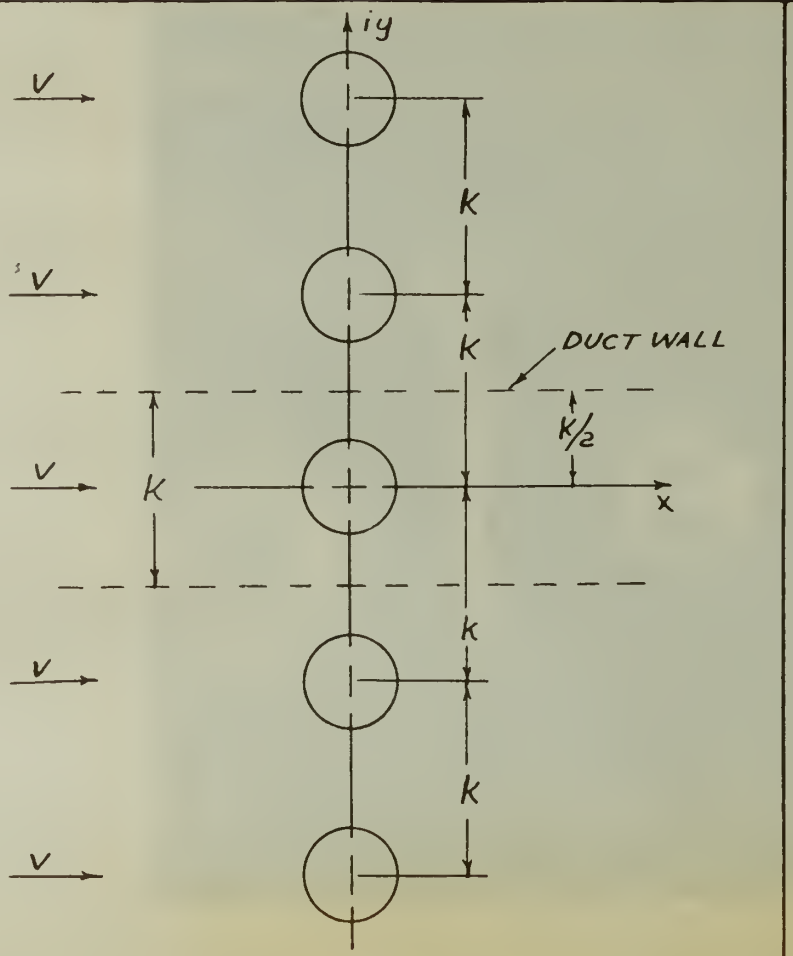

FIG. 3a STATIONARY CYLINDER AND IMAGES

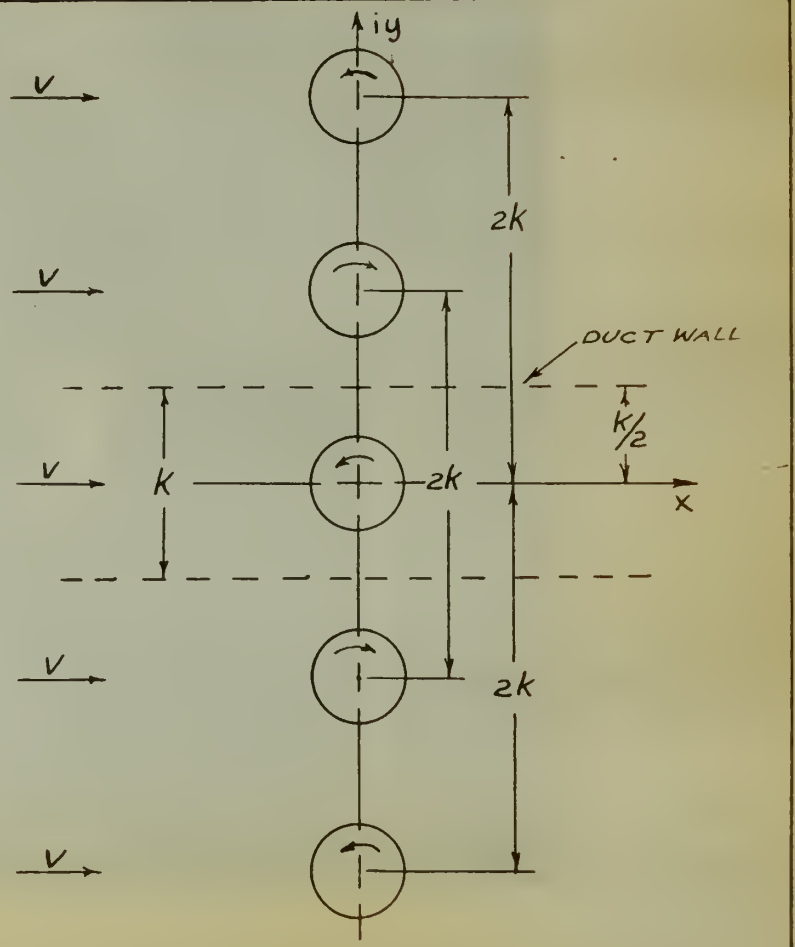

FIG. 3b VORTEX AND VORTEX IMAGES

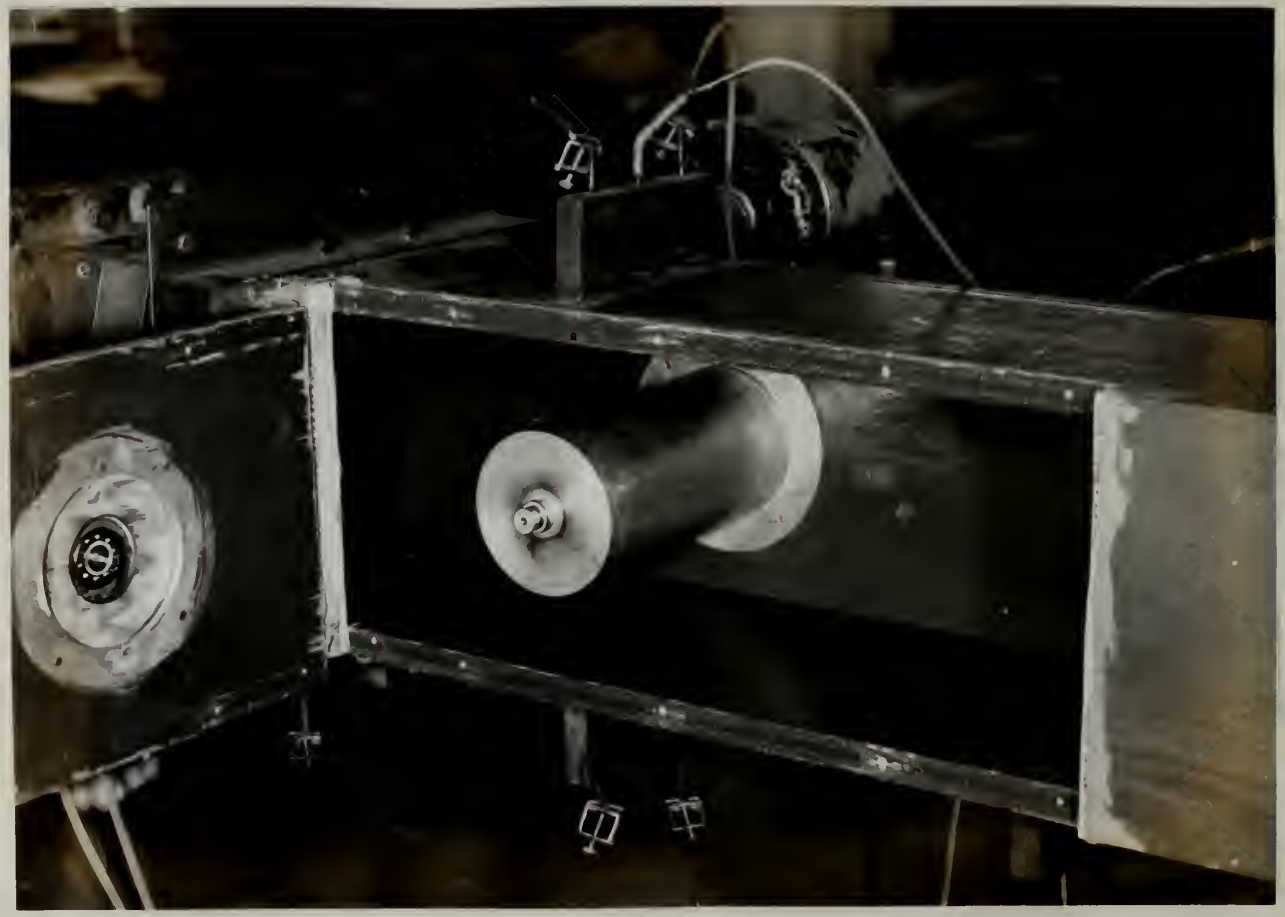

CUT AWAY VIEW OF FLOWMETER

FIG. 4

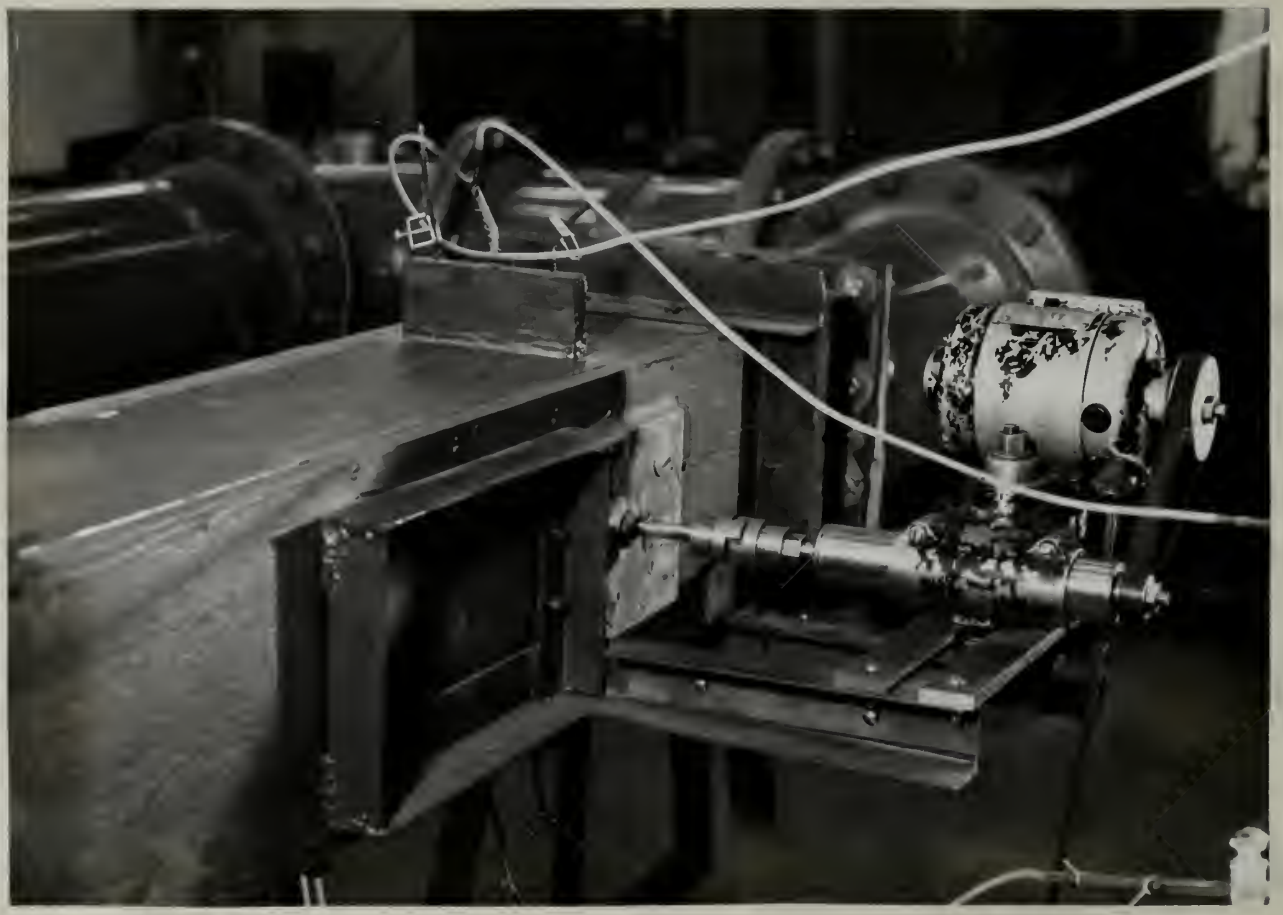

POWER DRIVE INSTALLATION

FIG. 5

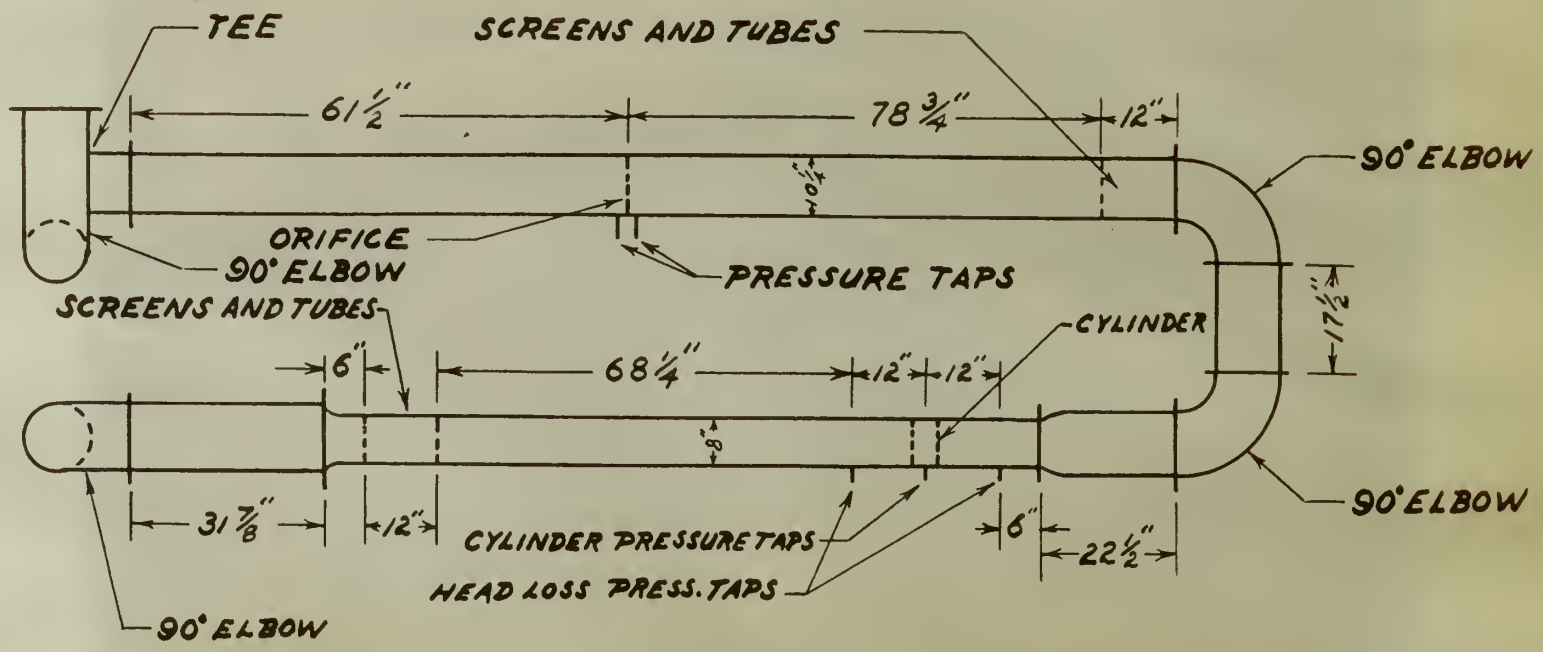

FIG. 6

PLAN VIEW	
TEST EQUIPMENT LAYOUT	
SCALE: 1"=32"	MAY 1951

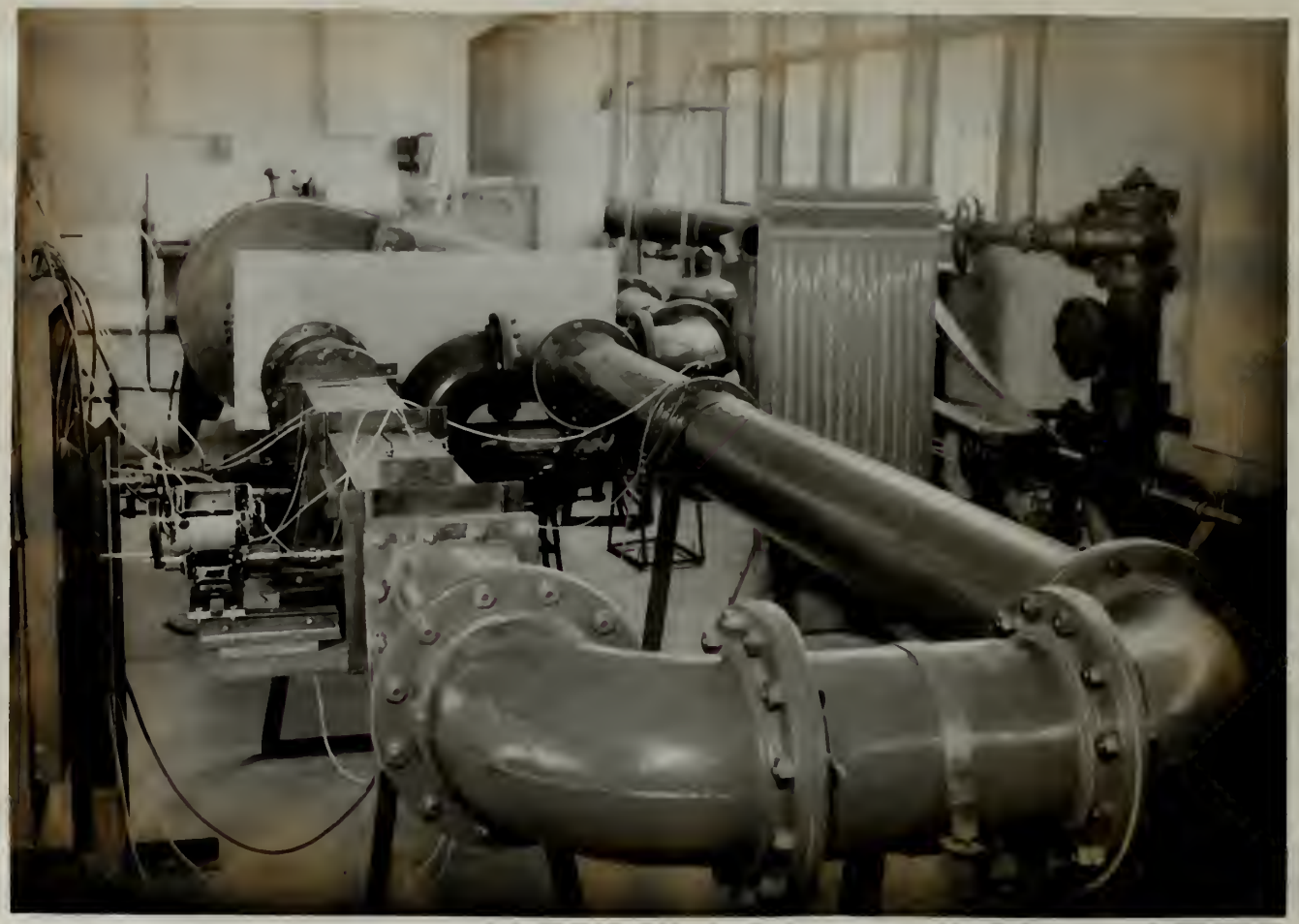

FLOWMETER TEST EQUIPMENT

FIG 7

INSTRUMENTATION

FIG. 8

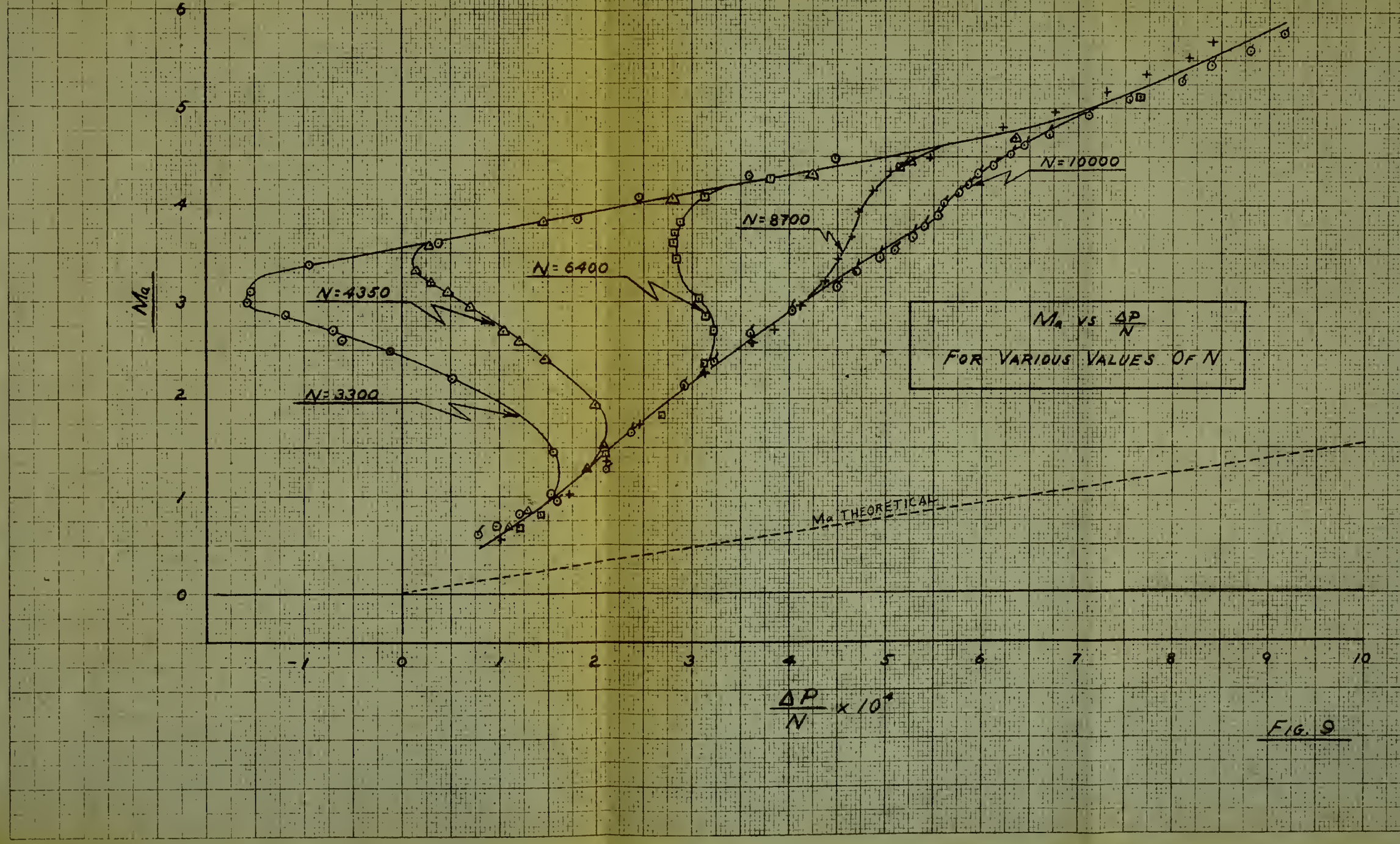
M_a
6
5
4
3
2
1
0
N=10000
N=8700
N=6400
N=4350
N=3300
M_a THEORETICAL
-1
0
1
2
3
4
5
6
7
8
9
10
$\frac{\Delta P}{N} \times 10^4$
M_a VS $\frac{\Delta P}{N}$
FOR VARIOUS VALUES OF N

FIG. 9

M_a vs $\frac{\Delta P}{N}$

THREE INDEPENDENT RUNS

N = 12000

△ MARCH 15, 1951

○ MARCH 19, 1951

□ MARCH 22, 1951

M_a THEORETICAL

M_a

$\frac{\Delta P}{N} \times 10^4$

0 1 2 3 4 5 6 7 8 9 10

0 1 2 3 4 5 6

FIG. 10

M_a VS. $\frac{\Delta P}{N}$

THREE INDEPENDENT RUNS

N = 14000

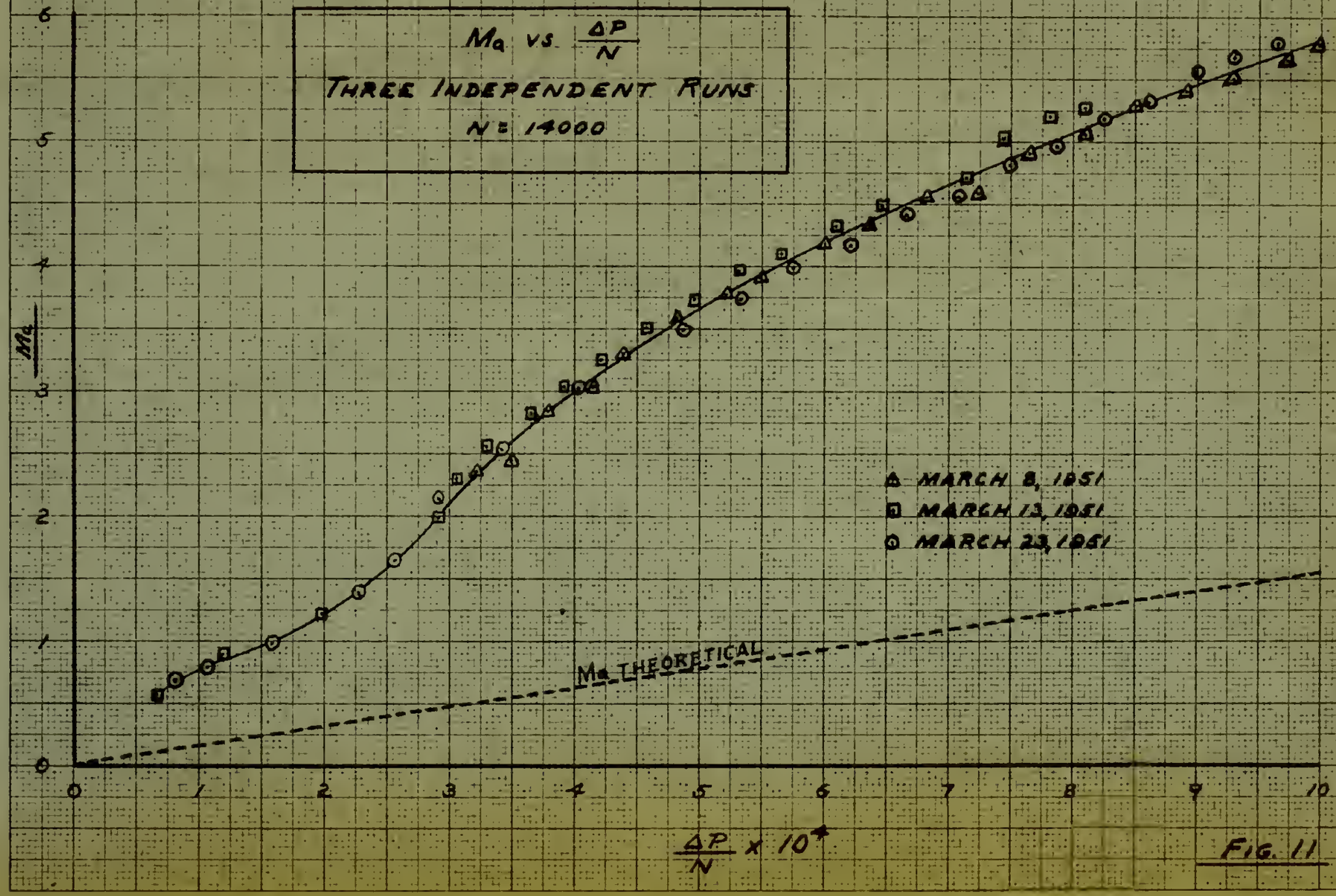

FIG. 11

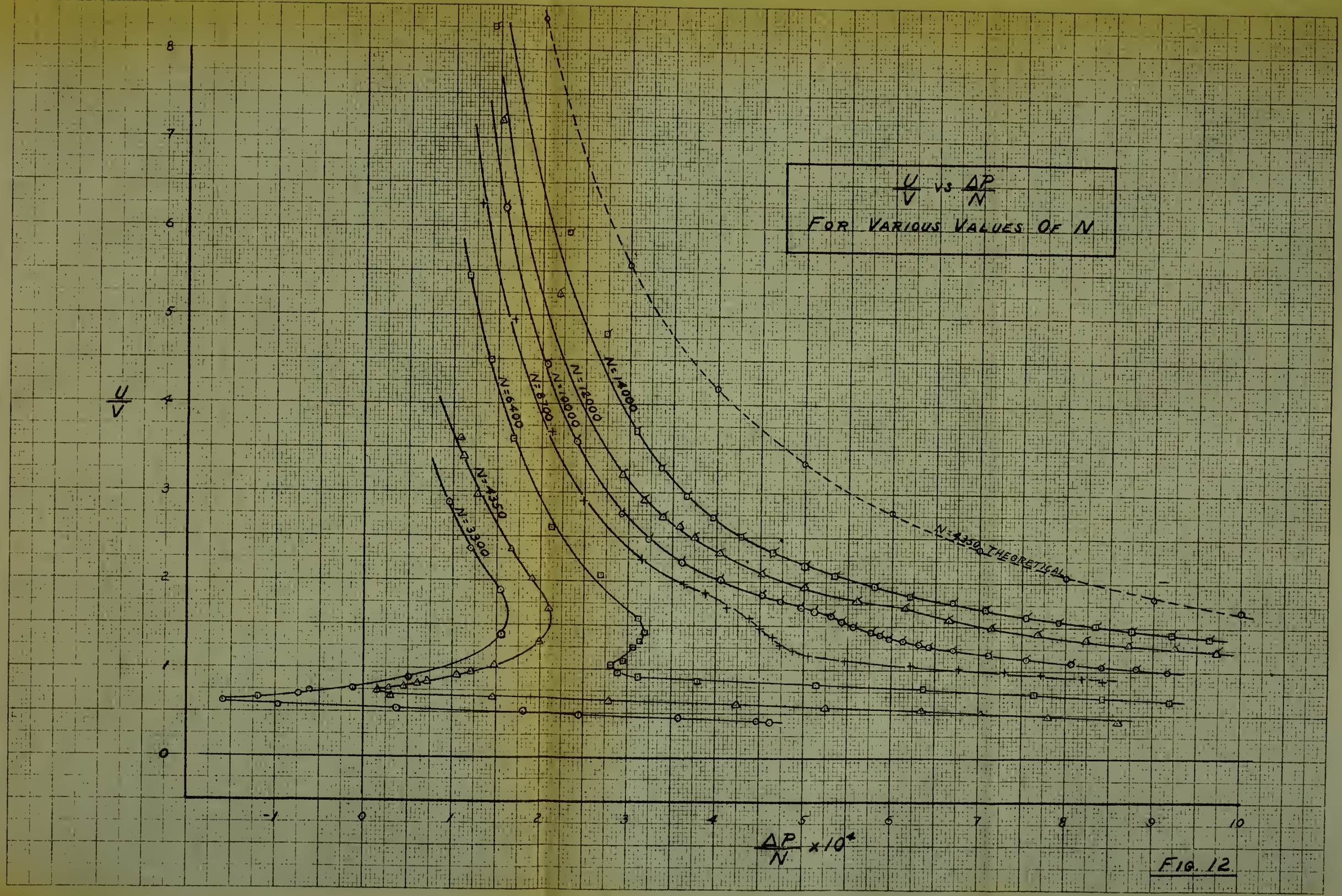
$\frac{U}{V}$ vs $\frac{\Delta P}{N}$
FOR VARIOUS VALUES OF N
$\frac{U}{V}$
$\frac{\Delta P}{N} \times 10^4$
N=14000
N=12000
N=10000
N=8700
N=6400
N=4350
N=3200
N=4350 THEORETICAL
0
1
2
3
4
5
6
7
8
9
10
-1

FIG. 12

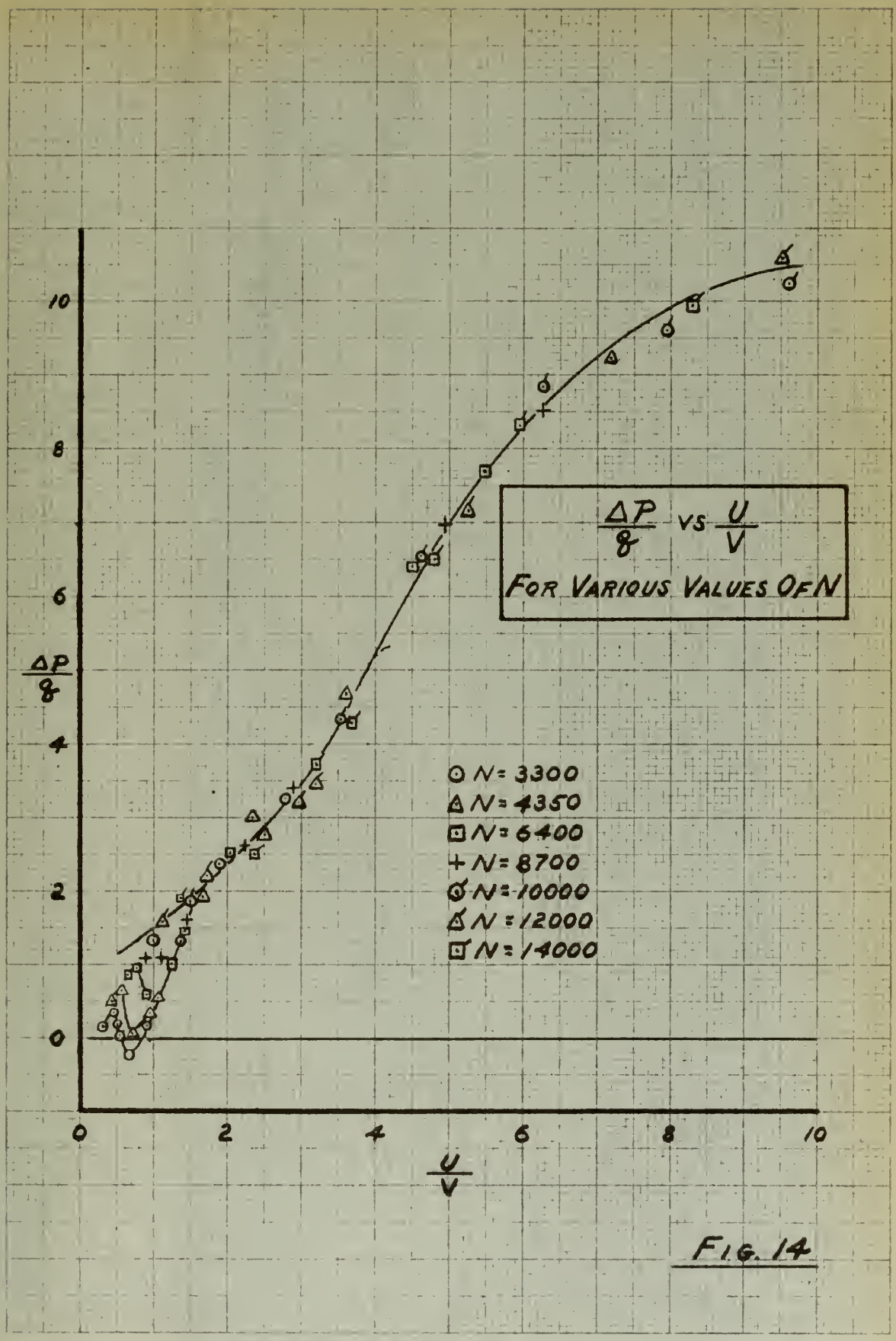
ΔP/g vs U/V
FOR VARIOUS VALUES OF N
○ N = 3300
△ N = 4350
□ N = 6400
+ N = 8700
◎ N = 10000
△ N = 12000
□ N = 14000
ΔP/g
U/V
0
2
4
6
8
10

FIG. 14

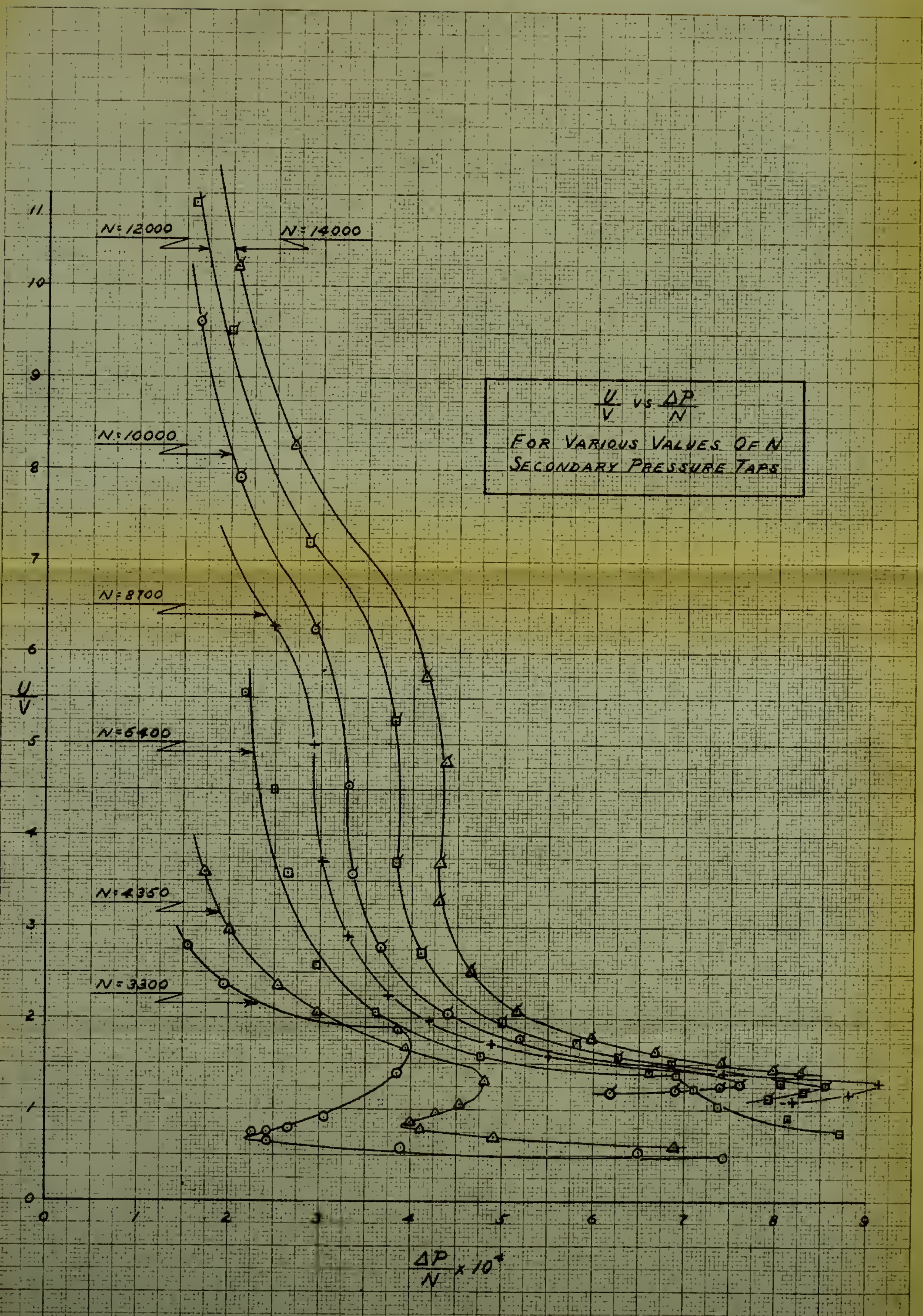

$\frac{U}{V}$ vs $\frac{\Delta P}{N}$

FOR VARIOUS VALUES OF N
SECONDARY PRESSURE TAPS

FIG. 15

PLATE 17

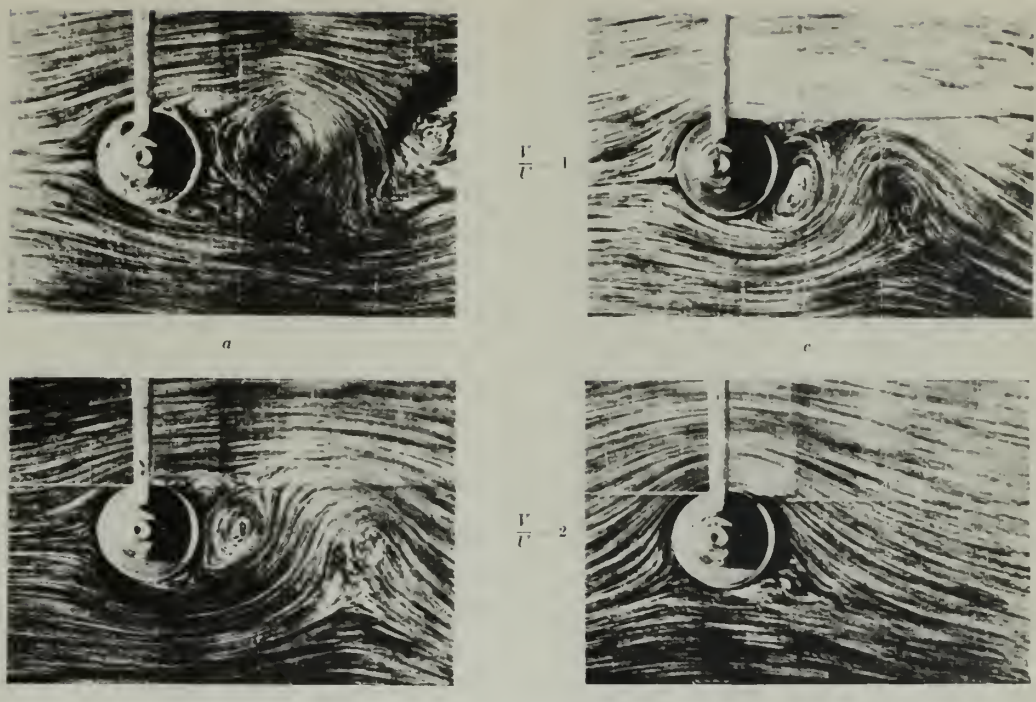

From L. Prandtl and O. Tietjens, *Hydro- und Aeromechanik*, 2 (Springer, Berlin)

V = CYL TANG. SPEED
U = STREAM VEL.

PLATE 18

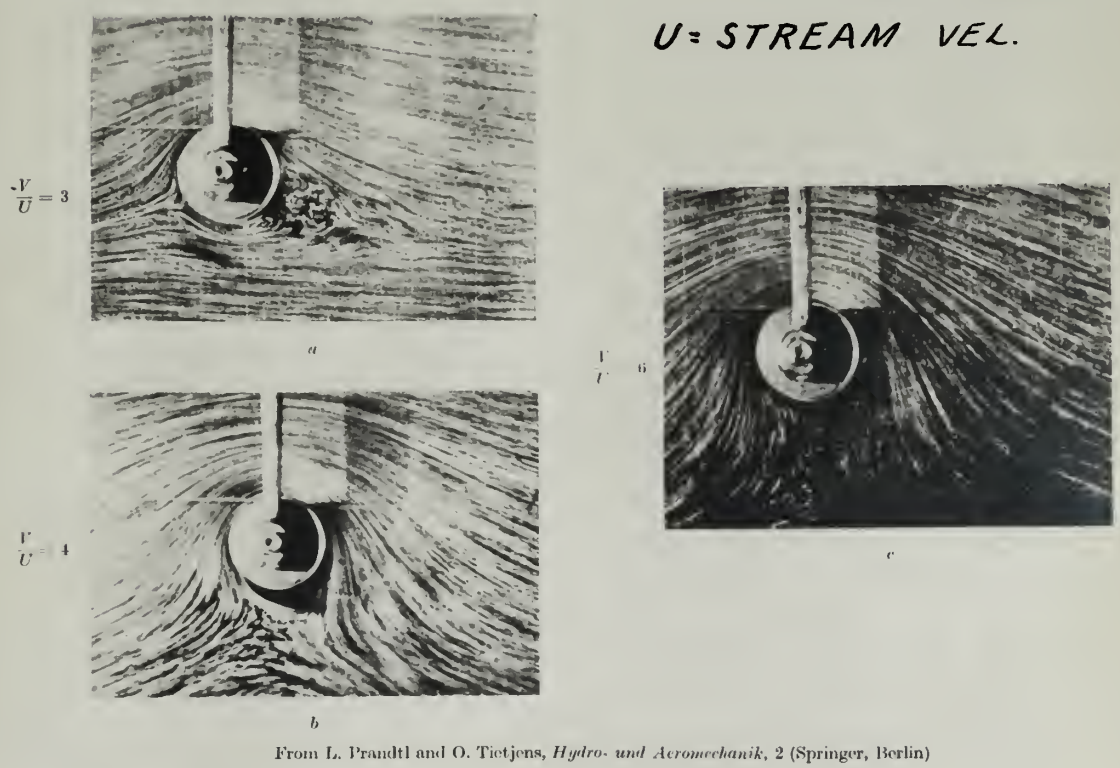

From L. Prandtl and O. Tietjens, *Hydro- und Aeromechanik*, 2 (Springer, Berlin)

FIG. 17

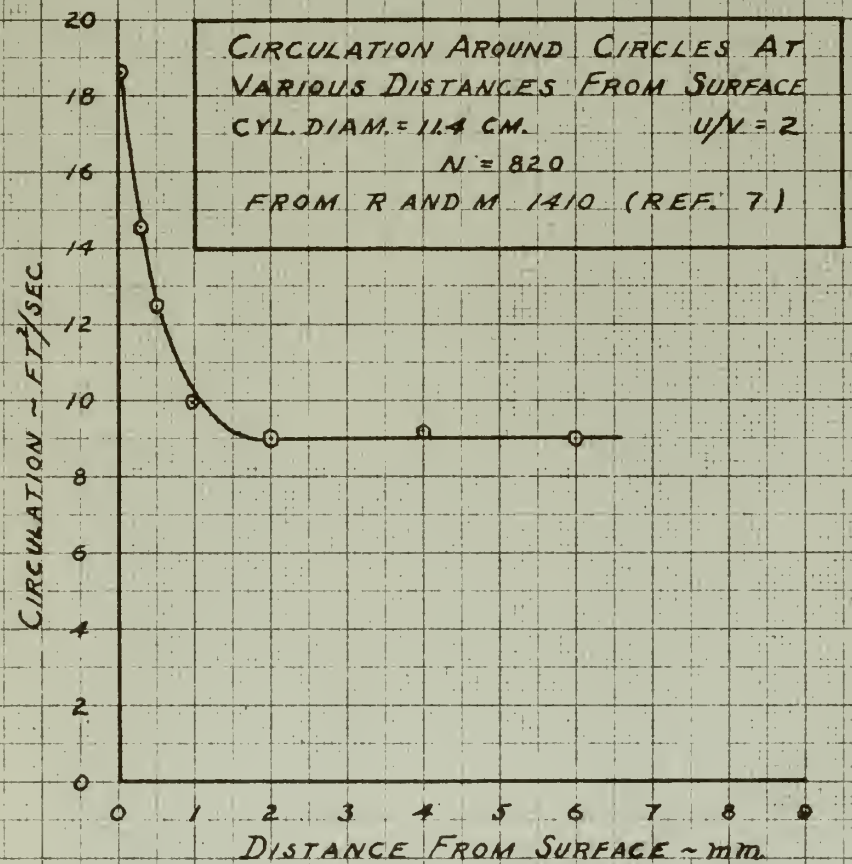
CIRCULATION AROUND CIRCLES AT VARIOUS DISTANCES FROM SURFACE
CYL. DIAM. = 11.4 CM. U/V = 2
N = 820
FROM R AND M 1410 (REF. 7)
CIRCULATION ~ FT²/SEC
0
2
4
6
8
10
12
14
16
18
20
0 1 2 3 4 5 6 7 8 9
DISTANCE FROM SURFACE ~ mm.

FIG. 18